DEPARTAMENTO DE CIÊNCIAS DA VIDA

FACULDADE DE CIÊNCIAS E TECNOLOGIA
UNIVERSIDADE DE COIMBRA

The role of miR-21 in the bone marrow microenvironment

Dissertação apresentada à Universidade de Coimbra para cumprimento dos requisitos necessários à obtenção do grau de Mestre em Biologia Celular e Molecular, realizada sob a orientação científica do Professor Doutor Sérgio Dias (Universidade de Lisboa) e do Professor Doutor Carlos Duarte (Universidade de Coimbra).

Celina Maria dos Reis Parreira

2013

Acknowledgements

First of all, I would like to express my gratitude to Doctor Sérgio Dias for accepting to be my supervisor and for giving me the opportunity to carry out my master dissertation with the excellent group that he coordinates. I am grateful for all the knowledge transmitted and for the confidence placed in me.

I would also like to thank my co-supervisor, Doctor Carlos Duarte, for the understanding and interest and also the commitment dedicated to the master in Cellular and Molecular Biology.

I would like to thank the coordinator of the master in Cellular and Molecular Biology, Doctor Emília Duarte, for her commitment to the course and also for her willingness and useful discussions.

I thank all my colleagues from the laboratory, for all the transmitted knowledge, support, help, advices and good moments shared in the lab. I want to thank specially Joana Afonso who was always available to help me, for the encouragement, friendship, confidence and the knowledge shared with me.

I would also like to thank my master colleagues, especially João, Andreia and Raquel, for the share of difficulties throughout this year.

I would like to thank my friends for the support, advices, smiles, everything. To those who, despite being far away, have always been close. I want also to thank people of *Republica77*, especially Patrícia, Sandra e Fernas, for all the good moments, friendship, complicity and support.

À minha família, um agradecimento muito especial por tudo. Aos meus tios e primos e aos meus avós pela compreensão, confiança e apoio que sempre me deram. Não posso também deixar de agradecer ao meu irmão, Nuno, pelo companheirismo, apoio, preocupação e pelas brincadeiras.

Aos meus pais pelas oportunidades que me deram, por acreditarem em mim, pela força e apoio incondicionais, por serem o meu "porto" seguro. Obrigada por tudo, principalmente pelos valores e sábios conselhos.

Index

Illustrations Index

Figures

Tables

Abbreviations

3’/5’UTR – 3’/5’Untranslated Region

ANXA1 – Annexin A1

CAM – Cell Adhesion Molecule

Ct – Threshold Cycle

EBM-2 - Endothelial Cell Basal Medium-2

ECM – Extracellular Matrix

ERK1/2 – Extracellular signal-Regulated Kinase 1/2

FBS – Fetal Bovine Serum

FGF2 – Fibroblast Growth Factor 2

FGFR1 – Fibroblast Growth Factor Receptor 1

HUVEC – Human Umbilical Vein Endothelial Cell

ICAM1 – Intercellular Adhesion Molecule 1

IL-8/15/21 – Interleukin-8/15/21

JAM – Junction Adhesion Molecule

MAPK – Mitogen-Activated Protein Kinase

PI3K – Phosphoinositide 3-Kinase

PIP_3 – Phosphatidylinositol (3,4,5)-Trisphosphate

pri-miRNA – primary micro Ribonucleic Acid

PTEN – Phosphatase and Tensin Homolog

RECK – Reversion-inducing Cysteine-rich protein with Kazal motifs

RhoB – Ras Homolog gene family, member B

Sc – Scramble

SDF-1 – Stromal cell-Derived Factor 1

Spry1/2 – Sprouty1/2

TGFβ – Tumor Growth Factor β

TGFβR – Tumor Growth Factor β Receptor

TSP-1 - Thrombospondin1

VCAM1 – Vascular Cell Adhesion Molecule 1

VE-Cadh – Vascular Endothelial-Cadherin

VEGF – Vascular Endothelial Growth Factor

VEGFR2 – Vascular Endothelial Growth Factor Receptor 2

VE-PTP – Vascular Endothelial-Protein Tyrosine Phosphatase

Abstract

Endothelial cells coat all the blood vessels, being essential for blood pressure regulation, blood coagulation, adhesion and transmigration of inflammatory cells from the vessels into the target tissue, and angiogenesis[1,2]. Although their properties and functions vary somewhat between species, organs, and depend on the location, size and type of vessel[1,3], all endothelial cells support the needs of the various adjacent cells and microenvironments. They are potential producers of angiocrine factors that are endothelial-derived factors with paracrine effects[4].

Among other molecules, microRNAs (miRNAs or miRs) regulate several biological processes in cells, including in endothelial cells. MicroRNAs are endogenous, single strand, non-coding short ribonucleic acid molecules (about 22 nucleotides) that regulate gene expression at post-transcriptional level. These molecules silence gene expression through binding to the target mRNA, inhibiting its translation into proteins or promoting mRNA degradation. MiRNAs present an important tissue- and cell-type-specific pattern and, by modulating gene expression, they may interfere with important processes such as apoptosis, cell proliferation and angiogenesis[5].

MiR-21 is an oncomiR, a miRNA that acts like an oncogene. It belongs to the specific miRNA signature of the vasculature[6] and is overexpressed in various solid tumors[7]. It is described that this particular molecule is involved in cell survival, proliferation, motility, invasion, metastasis and chemoresistence[7,8]. However, its role in bone marrow remains to be elucidated.

Aiming to evaluate the role of miR-21 in the bone marrow microenvironment and in bone marrow endothelial cells in particular, miR-21 expression was investigated on bone marrow cells. Moreover, the modulation of miR-21 levels in endothelial cells and the gene expression analysis through real-time quantitative polymerase chain reaction (RT-qPCR) allowed the identification of downstream targets underlying miR-21 regulation of angiogenesis. Bioinformatic tools and literature allowed the choice of 9 predicted targets, from which phosphatase and tensin homolog (PTEN) and Sprouty2 were confirmed to be regulated by miR-21. Phenotypic changes modulated by miR-21 levels were also assessed, indicating that miR-21 promotes tubulogenesis in the presence of vascular endothelial growth factor or basic fibroblast growth factor.

Key words: endothelial cell, angiogenesis, miRNA, miR-21

Resumo

As células endoteliais revestem os vasos sanguíneos, apresentando um papel essencial na regulação da pressão arterial, na coagulação do sangue, na adesão e transmigração de células envolvidas no processo inflamatório do lúmen dos vasos para o tecido alvo, e na angiogénese[1,2]. Apesar da heterogeneidade das suas propriedades e funções entre espécies, órgãos, e dependendo da localização, tamanho e tipo de vaso sanguíneo[1,3], todas as células endoteliais apoiam as necessidades das células adjacentes e do microambiente que as rodeia. São potenciais produtoras de factores angiócrinos, que são factores derivados das células endoteliais com actividade parácrina[4].

Entre outras moléculas, os microRNAs (miRNAs ou miRs) regulam vários processos biológicos, actuando ao nível das células, nomeadamente das células endoteliais. Os microRNAs são pequenas moléculas de ácido ribonucleico de cadeia única não codificante (cerca de 22 nucleótidos), que regulam a expressão génica ao nível pós-transcripcional. Estas moléculas endógenas inibem a expressão génica ligando-se ao mRNA alvo, impedindo a sua transcrição em proteínas ou promovendo a sua degradação. Os miRNAs apresentam um padrão específico consoante o tipo de célula ou tecido e, através da modulação da expressão génica, podem interferir com importantes processos biológicos, tais como a apoptose e proliferação celulares e a angiogénese[5].

O miR-21 é um oncomiR, isto é, um miRNA que actua como oncogene. Pertence à assinatura de miRNAs específica do sistema vascular[6] e está sobrexpresso em vários tumores sólidos[7]. Esta molécula em particular está descrita como estando envolvida na sobrevivência, proliferação e mobilidade celular, bem como nos processos de invasão, metástase e resistência à quimioterapia[7,8]. Contudo, o seu papel na medula óssea continua por esclarecer.

Com o objectivo de avaliar o papel do miR-21 no microambiente da medula óssea e nas células endoteliais da medula óssea em particular, a expressão do miR-21 foi estudada nas células da medula óssea. Além disso, através da modulação dos níveis do mir-21 nas células endoteliais e a análise da expressão génica por reacção em cadeia da polimerase em tempo real quantitativa (RT-qPCR) permitiram a identificação de possíveis alvos do miR-21 envolvidos na regulação da angiogénese. A utilização de ferramentas bioinformáticas em conjunto com a literatura facilitou a escolha de 9

possíveis alvos, dos quais PTEN e Sprouty2 demonstraram ser regulados pelo mir-21. Alterações fenotípicas derivadas da regulação deste miRNA também foram analisadas e indicam que miR-21 promove a tubulogénese na presença do factor de crescimento endotelial vascular e do factor de crescimento fibroblástico básico.

Palavras chave: células endoteliais, angiogénese, miRNA, miR-21

Introduction

Blood vessels and endothelial cell properties

The circulatory system is the first to develop during the vertebrate gestation, to guarantee the delivery of nutrients and oxygen and to assure the removal of metabolic waste from all the cells and tissues of the growing embryo. While the embryo grows through cell differentiation and morphogenesis, also the vasculature spreads out, remodels and differentiates into different types of blood vessels[1].

The first stage of vascular development, vasculogenesis, begins after gastrulation, with de novo emergence of primordial endothelial cells from the coalescence of blood islands of the mesoderm, in the extraembryonic yolk sac, to form a primary vascular plexus. Afterwards, this vascular plexus remodels to form a highly differentiated circulatory network, through angiogenesis, the process by which new blood vessels sprout from preexisting ones[1].

1. Blood vessels

Blood vessels are highly organized and complex structures, proficient to control blood flow. Their integrity is assured by endothelial cells, pericytes, smooth muscle cells, fibroblasts, glial cells and inflammatory cells and by the extracellular matrix (ECM), which bears the constant mechanical forces exerted by the blood flow, controls the proliferation and differentiation of the vascular cells and modulates the effects of growth factors[1,9]. Blood vessels may be subdivided into 3 main interconnected types, differing in structure and function[1,10,11]:

1. The arteries that have the vital function of conducting oxygenated blood all over the body, with the exception of the pulmonary arteries that carry deoxygenated blood to the lungs. They are constituted by an inner monolayer (*tunica intima*) of endothelial cells, a middle layer (*tunica media*) of thick connective tissue with elastin filaments and smooth muscle cells, and an outer layer (*tunica adventitia*) of fibrous connective tissue, containing fibroblasts, parasympathetic nerves, that foster the smooth muscle of the middle layer to sustain the high blood pressure, and collagen, that supports the vessel and links it to the surrounding tissues. All 3

layers are separated by elastic lamina and have collagen in their constitution, acting like an anchor to all the cells. Arteries have narrow lumen, contributing to the optimal blood flow. When they reach organs, they divide themselves into smaller vessels, the arterioles, which in turn give rise to capillaries by division as well[10,11].

2. The capillaries that are the tiniest vessels, composed only by a single cell layer of endothelial cells surrounded by a basal lamina consisting mostly of type IV collagen. At this level, there is very low blood pressure to allow the gaseous and nutritional exchange between capillaries and tissue fluids. The precapillary sphincters, bands of smooth muscle around arterioles, control the quantity of blood flowing into a capillary[10,11].
3. The veins that, with the exception of the pulmonary ones, carry the deoxygenated blood from the organs back to the heart. They are also composed by three layers similar to arteries, but they have a much thinner middle muscular layer and a much larger lumen. Besides, they are fitted with one-way valves, derived from the endothelium, to prevent the backflow of blood, due to the tiny blood pressure in these vessels[10,11].

2. Endothelial Cells

Therefore, all the blood vessels are coated by endothelial cells that are essential for blood pressure regulation, blood coagulation, adhesion and transmigration of inflammatory cells from the vessels into the target tissue, and angiogenesis[1,2].

Endothelial cells properties and functions vary somewhat between species, organs, and depend on the location, size and type of vessel[1,3]. All endothelial cells are highly metabolically active and have different phenotypes, supporting the needs of the various adjacent cells and microenvironments. However, they are usually thin and slightly elongated along the axis of the vessel, reducing the shear stress forces of the flowing blood[3].

The development and maintenance of the endothelium requires the establishment of a dynamic equilibrium between physical forces (e.g. tension, compression or shear stress), polarity, adhesion and permeability[12]. In addition, as described below, endothelial cell number and function is also tightly regulated by the action of pro- and anti-angiogenic growth factors. The quiescence of the adult normal vasculature is maintained by the tight equilibrium between these angiogenic

promoters and inhibitors, respectively. Pro-angiogenic factors like angiopoietins, basic fibroblast growth factor (bFGF) and vascular endothelial growth factor (VEGF) promote angiogenesis, inducing cell survival and migration. Anti-angiogenic factors, such as thrombospondins (TSPs), angiostatin and endostatin, suppress migration and induces apoptosis of endothelial cells. The disruption of this angiogenesis balance might result in physiological angiogenesis, such as wound healing, or in pathological angiogenesis, such as tumor angiogenesis[1,13,14].

2.1. Endothelial Cell Polarity

The polarity of the endothelium is defined by different phosphoinositides and protein complexes in apical and basolateral regions, corresponding to luminal and abluminal membranes, respectively. Modulation cell polarity occurs through changes in cell-cell junctional molecules. Par3, Par6 and atypical protein kinase C (aPKC) are the crucial proteins to this process. Par3 is associated to cell-to-cell junctions, while Par6 and aPKC defines the apical region. Crumbs and Scribble assure the stabilization of apical and basolateral domains, respectively, through their combination with the Par proteins. All these complexes associated to polarity are decisive for lumen formation as well[12,15].

2.2. Endothelial Cell Adhesion

Endothelial cells form a crucial selective semi-permeable barrier between the vessel lumen and the surrounding tissue, controlling the transport of small molecules, macromolecules and cells and the degradation of lipoprotein particles[1,2]. These barrier functions are highly dependent on the type of cell adhesion molecules (CAMs) that delineate cell borders, either cell-cell adhesions, which assure the barrier function, or cell-matrix adhesions, which assure barrier integrity (Figure 1)[16].

The major families of CAMs are cadherins, selectins, integrins and Ig-superfamily CAMs. Cadherins form homodimers, cluster together and their activity is calcium-dependent. Selectins form homodimers as well and their lectin domains recognize specialized sugar structures on glycoproteins on adjacent cells. Integrins form heterodimers and bind to very large multiadhesive matrix proteins, such as fibronectin, supporting the cell anchorage to collagen and proteoglycans. Ig-CAMs, in turn, do not form dimmers, but may have both homophilic and heterophilic interactions. Many

adhesion molecules interact with the cytoskeleton through adapter proteins, providing mechanical continuity among cells and allowing mechanical resistance to disruption. Thereby, these interactions are not only adhesive, but they also facilitate communication between cells and microenvironment[16].

All these CAMs are on the basis of the different types of connecting junctions that bind the cells together[17].

1. Gap junctions connect both cytosols joining two connexon hemichannels, constituted by six connexin molecules. The formed pore is very selective, only allowing water, ions, and small molecules to pass through. Thus, cell communication is the main function of this type of joint[17].
2. Tight junctions do not allow transition of large molecules through the extracellular space between the endothelial cells, sealing a barrier. They also sustain the polarity of these cells by preventing the diffusion of membrane proteins and glycolipids between the apical and the basolateral regions, maintaining different lipid composition of the two regions. Occludin, claudin and junction adhesion molecule (JAM) are the main proteins found in tight junctions. They combine with actin filaments, controlling solute flow and cell signaling[17].
3. Anchoring junctions attach cells mechanically within the tissue and to the ECM. Several types of these junctional complexes serve this function:
    2.2. Adherent junctions are carried out by cadherins, which binds to p120-catenin and β-catenin, which interacts with α-catenin, which, in turn, binds to F-actin. Adherent junctions tie cells not only to other cells, but also to the ECM and, simultaneously, they act as a signaling platform[17,18].
    2.3. Desmosomes are similar to adherent junctions, although they bind to intermediate filaments. They are composed by desmoglein and desmocollin, transmembranar proteins that belong to cadherin family, and they also require attachment to a cytoplasmic plaque. The cytoplasmic plaque is formed by plakoglobin, desmoplakins and plakophilins that are structures similar to α-catenin and β-catenin. Desmosomes confer strength and durability to the cells[17].
    2.4. Hemidesmosomes, in contrast to all the other types of junctions, are involved only in the anchorage of the cells to the ECM through the attachment of integrins to specific ligands, like ECM proteins, such as fibronectin, fibrinogen, vitronectin, and collagen. This interaction manages cell shape, rigidity and signaling[18,19].

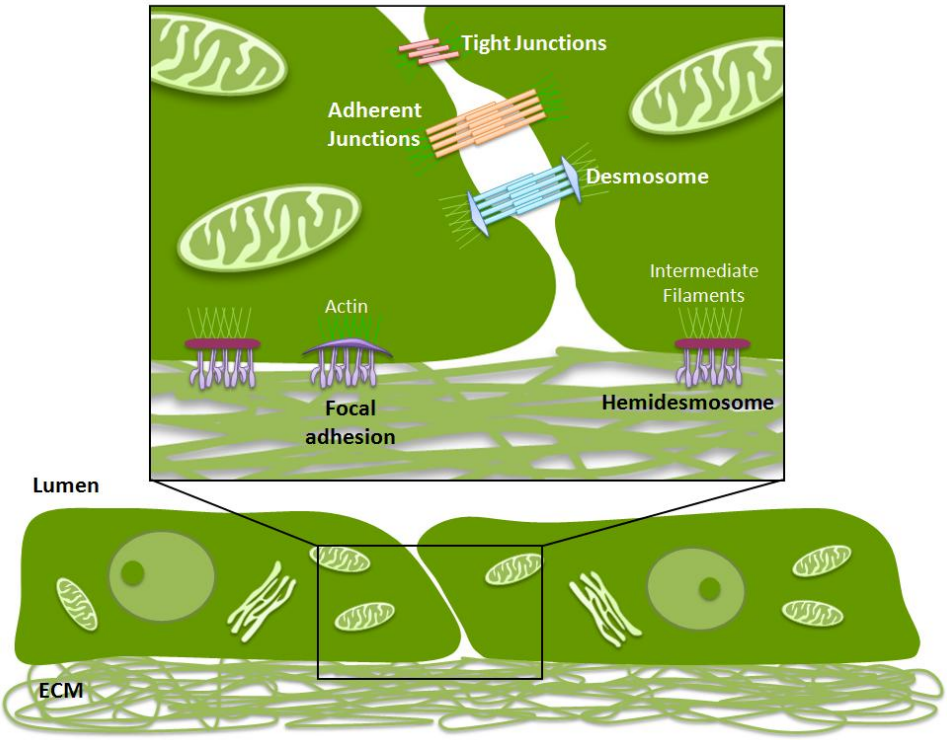

Figure 1 – Schematic representation of endothelial cell adhesion.

2.2.1. Cell-to-cell Junctions

Endothelial cells are joined together by transmembranar adhesive proteins that, beyond the adhesion function, are responsible for intercellular recognition and might indirectly regulate transcriptional activity, once they may transmit several signals to the cell, controlling several physiological features. These molecules must be very dynamic to allow leukocyte transmigration during inflammation and cellular remodeling during angiogenesis, confining paracellular permeability[20].

Cell-to-cell connections are maintained essentially by tight junctions and adherent junctions, with specific positions in the junctional cleft. The tight junctions cover the most apical position, sealing the cleft limits on the way to the luminal surface. The adherent junctions, in turn, are localized more basally, sustaining the morphology and stability of the endothelium. Even so, they can crosstalk[16,20].

In spite of all the adhesion molecules present in endothelial cells, only a few are endothelial specific: claudin-5 in tight junctions and vascular endothelial (VE)-cadherin and vascular endothelial-protein tyrosine phosphatase (VE-PTP) in adherent junctions[20].

The major component of adherent junctions is VE-cadherin, an endothelial specific and calcium-dependent glycoprotein, which is very dynamic and sensitive to extracellular stimuli. It may directly or indirectly stimulate signaling pathways in the cells[18]. VE-cadherin may form complexes with vascular endothelial growth factor receptor (VEGFR)2 and with transforming growth factor β receptor (TGFβR) I and II. Their ligands, VEGFA and TGFβ, respectively, trigger endothelial differentiation, growth and stabilization. In response to VEGFA, the VE-Cadherin-VEGFR2 complex activity prevents apoptosis and promotes cell stability through activation of Akt, while inhibits cell cycle mediated by p42/44 mitogen-activated protein kinase (MAPK). The VE-cadherin-TGFβR complex also promotes vessel stabilization, inhibiting endothelial proliferation and migration in response to TGFβ[20].

Another important complex in stable vessels is Tie2-VE-PTP. Tie2 is a tyrosine kinase receptor that sustains cell quiescence and stabilization in response to its ligand, Angiopoietin1 (Ang1), which is produced by the pericytes. Besides Tie2, VE-PTP can also combine with VE-cadherin, although it is not known if these interactions are mutually exclusive or not[20].

2.2.2. Cell-to-matrix Junctions

The ECM is fundamental for the endothelial barrier function and, in general, is composed by collagen, others glycoproteins and proteoglycans. It is the diversity and the amount of these components that portray different tissue-specific ECMs[19].

The endothelial cells are provided with integrins, which are bound to the ECM in restrict locals called “focal adhesions”. Each integrin is a heterodimer resulting from a unique combination of α- and β-subunits. These subunits are type I transmembranar glycoproteins with a small cytoplasmic domain and a large extracellular domain[19]. Integrins bind to the Arg-Gly-Asp (RGD) sequence of ECM proteins such as fibronectin, fibrinogen, vitronectin, and collagen. Their cytoplasmic domain interacts with actin-binding proteins, such as vinculin, α-actinin, paxillin and talin. These interactions influence cell morphology and paracellular permeability[19].

In the migration process, integrins are recycled by caveolae, a special type of lipid raft invaginations that mediate integrin interactions with Rho GTPases. Thereby, integrins activate Rho GTPases, like RhoA, Rac1 and Cdc42, inducing membrane protrusion[14].

2.3. Endothelial cells proliferation and apoptosis

During vascular plexus remodeling and in response to angiogenic stimuli, endothelial cells proliferate, migrate and coalesce. Their proliferation must be tightly regulated to reach proper architecture, stability and function of an expanding vascular network. As endothelial cells become more specialized and the circulatory system is completely created, these cells decrease gradually their proliferation rate. Hence, mature endothelial cells have a low proliferative rate, except in angiogenesis, and a low apoptotic rate, except in disease[1,14].

The cell survival and proliferation is induced mainly by the phosphoinositide 3-kinase (PI3K)/Akt signal transduction cascade. This signaling pathway is strongly regulated by phosphatase and tensin homolog (PTEN), a well-known tumor suppressor protein. PTEN suppresses Akt activity through the dephosphorylation of the phosphatidylinositol (3,4,5)-trisphosphate (PIP_3), which is required to Akt activation. Akt, also known as protein kinase B, is a serine/threonine-specific protein kinase with a role in several cellular processes like translation initiation, cell growth, glycogen synthesis, cell cycle, proliferation and apoptosis[21].

In normal conditions, Akt phosphorylates p21 and p27 cyclin-dependent kinase (Cdk) inhibitors, leading to their cytosolic localization, promoting the cell cycle. In addition, Akt phosphorylates procaspase-9, decreasing its protease activity, and Bcl-2-associated death promoter (BAD) protein, hence inhibiting apoptosis. However, when PTEN is overexpressed, the activity of Akt is inhibited, inducing apoptosis, suppressing cell cycle and promoting the increase of p53 levels, enhancing the transcription of several genes such as PTEN and p21[21,22].

3. Angiogenesis

Angiogenesis is a highly regulated process for the forming vasculature to have the proper integrity and patterning. It may occur through endothelial sprouting or through non-sprouting intussusceptive microvascular growth (IMG)[1,20].

The endothelial sprouting (Figure 2) involves the loss of junction contacts between the endothelial cells, degradation of the basement membrane by proteases and migration of tip cells in reaction to angiogenic stimuli, such as VEGF, even if not all the exposed endothelial cells respond to the proangiogenic signals[1,14,20]. Notwithstanding, recent data go against the immutably of tip and stalk cells and

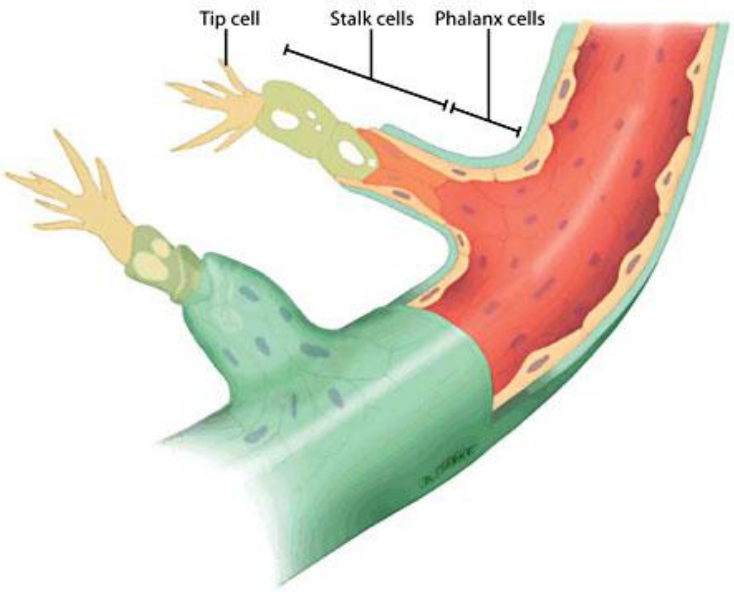

Figure 2 – Schematic representation of sprouting angiogenesis. Adapted from De Spiegelaere W, Casteleyn C, Van den Broeck W, Plendl J, Bahramsoltani M *et al*. Intussusceptive angiogenesis: a biologically relevant form of angiogenesis. *J Vasc Res*. 2012; 49(5): 390-404.

demonstrate that there is a dynamic arrangement of cells that change position frequently within a growing vascular sprout, through interchangeable adhesions between cells and the ECM[14].

The IMG (Figure 3) consists in the insertion of several transcapillary pillars by a process known as intussusception, increasing capillary network and complexity[1,20].

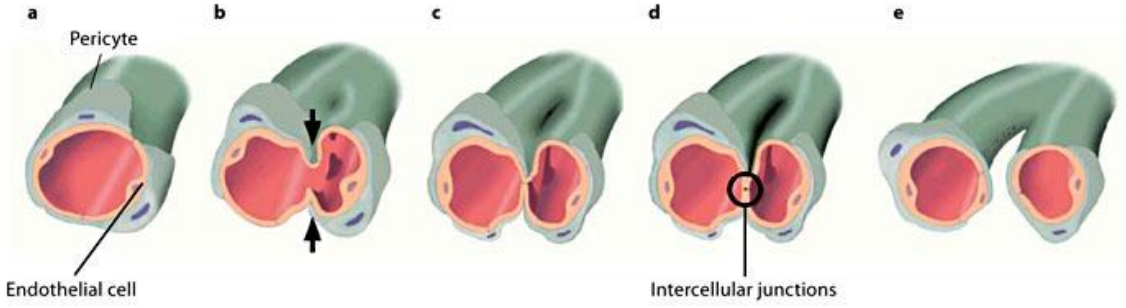

Figure 3 – Schematic representation of the intussusceptive microvascular growth. Adapted from De Spiegelaere W, Casteleyn C, Van den Broeck W, Plendl J, Bahramsoltani M *et al*. Intussusceptive angiogenesis: a biologically relevant form of angiogenesis. *J Vasc Res*. 2012; 49(5): 390-404. (a) The opposite walls of the capillary start to migrate to each other, (b,c) a intraluminal pillar is formed and (d) the cell-to-cell junctions are established. (e) The further growth of this pillar forms two new vessels from the original one.

Bone marrow vessels: "instructors" of hematopoietic function

Several studies suggests that endothelial cells are not just a barrier between the vessel lumen and surrounding tissue that controls the traffic of cells and molecules, but also potential producers of stem cell and progenitor cells active angiocrine factors[4].

The angiocrine factors are paracrine released endothelial-derived factors. These may be growth factors, trophogens, adhesion molecules as intercellular adhesion molecule 1 (ICAM1), vascular cell adhesion molecule 1 (VCAM1), E-selectin, P-selectin and hyaluronan, and chemokines as interleukin (IL)-8, monocyte chemoattractant protein 1 (MCP-1) and stromal cell-derived factor 1 (SDF1). The angiocrine factors have a key role in tissue repair, enhanced after treatment with anti-angiogenic and chemotherapeutic agents or radiotherapy. By modulating the proliferation of stem and progenitor cells[23], some of these particular factors, that might support hematopoiesis but not tumorigenesis, improve bone marrow recovery, mitigating the chemotherapy and irradiation effects[4].

It is thought that the vascular niche within each organ is scheduled to fill the physiological requirements of a certain tissue, suggesting an organ-specific regulation of the expression of angiogenic factors[24]. Endothelial cells might be therefore considered instructive organ-specific vascular niches, since that they control the maintenance and the reconstitution of stem and progenitor cells through secretion of specific angiocrine factors and deposition of ECM[4].

A recent study demonstrate that direct cellular interaction with endothelial cells control the fate of hematopoietic stem and progenitor cells (HSPCs) and that the equilibrium between proliferation of long-term hematopoietic stem cells (LT-HSCs) and lineage-specific differentiation of HSPCs is due to the differential recruitment of Akt and mitogen-activated protein kinase (MAPK) signaling pathways in endothelial cells. Both pathways act upregulating distinct angiocrine factors. Akt-activated endothelial cells induce the expression of HSPC-active angiocrine factors by the action of mTOR and favor the self-renewal of LT-HSCs and the proliferation of HSPCs. On the other hand, MAPK co-activation promotes maintenance and lineage-specific differentiation of HSPCs. These both processes are fundamental during hematopoiesis recovery to ensure not only the differentiation of the HSPCs, but also the LT-HSC self-renewal[24].

Another recent study shows that liver sinusoidal endothelial cells (LSECs) initiate and support liver regeneration after a 70% partial hepatectomy. It had been further proved that VEGF-A receptor-2 (VEGFR2) and the subsequent endothelial cell-specific transcription factor *Id1* are crucial for the proliferation and recovery of the hepato-vascular mass due to lack of LSEC-derived angiocrine factors, such as hepatocyte growth factor (HGF)[25]. It is likewise described that pulmonary capillary endothelial cells (PCECs) proliferate after unilateral pneumonectomy (PNX), favoring alveologenesis through the intermediary of VEGFR2 and fibroblast growth factor receptor 1 (FGFR1) and subsequent matrix metalloproteinase 14 (MMP14)[26].

Thereby, vascular derived-tumor specific angiocrine factors may be huge potential therapeutic targets fighting against cancer, since this is a targeted strategy that reduces therapy-induced vascular toxicity[4].

However, even though the evidences of the production of stem cell active factors such as bone morphogenetic protein 2 (BMP2), BMP4, tumor growth factor β (TGFβ), brain-derived neurotrophic factor (BDNF), jagged 1 and jagged 2 and angiogenic factors such as placental growth factor (PGF), angiopoietin2 (Ang2), VEGFA, fibroblast growth factor 2 (FGF2) and platelet-derived growth factor (PDGF) by endothelial cells that sustain organogenesis, tissue recovery and even tumorigenesis, the exact identity of the organ-specific angiocrine factors is not known yet[4].

MicroRNAs

MicroRNAs (miRNAs) are an abundant class of endogenous, short (20 to 25 nucleotides in length), highly conserved, non-coding ribonucleic acid molecules. They have a tissue- and cell-type-specific pattern and are important regulators of gene expression at post-transcriptional level that have been shown to control a wide range of biological functions such as cellular proliferation, differentiation, metabolism and apoptosis[5,27].

1. miRNA biogenesis and mechanism of action

miRNAs are transcribed from an individual miRNA gene, from an intron of a coding or non-coding gene or even from polycistronic transcripts. Additionally, this particular class of endogenous small RNA molecules may have their own promoters, being expressed in an independent way or, if organized in clusters, they share the same transcriptional regulation[5,27].

As shown in Figure 4, the long primary transcript generate a stem-loop conformation, called primary miRNA (pri-miRNA), which is processed by Drosha, a ribonuclease III (RNase III), together with DGCR8, a molecular anchor necessary for the recognition of pri-miRNA. An alternative pathway may occur to bypass the cleavage step from Drosha, if the miRNA derives from intronic hairpins, being called mirton. In this case, spliceosome acts like Drosha processing pri-miRNA. After this nuclear processing into stem-loop precursor (pre-miRNA), this is subsequently transported to the cytoplasm by Exportin-5 in a Ran-GTP-dependent manner. Once in the cytoplasm, Dicer, another RNase III, cleaves the pre-miRNA to produce the mature ≈22 nucleotide miRNA duplex, which is incorporated as single-stranded RNAs into the effector RNA-induced silencing complex (RISC). The miRNA duplex is unwound into the mature guide strand and its complementary passenger strand, which is mostly degraded. The process by which the cell selects one strand of the double strand miRNA is really unknown. Included in RISC, whose key components belong to Argonaute (Ago) family, guide strand miRNA conducts the complex to its target RNA. The mature miRNA binds to the target mRNA coding sequences or to the 5’ or 3’-untranslated regions (UTR) by Watson-Crick base pairing with the help of RISC. However, most of the predicted and experimentally characterized miRNA sites are positioned in the mRNA 3’UTR. This

interaction leads to translational repression in cases of low miRNA-target complementarity or to mRNA degradation whether this interaction is perfect or near-perfect. It is noted that various miRNAs may cooperatively bind to the same 3'UTR and that each miRNA may regulate multiple targets[5,6,27,28]. Cells may further exchange miRNAs between them via exosomes, producing biological effects close by or at a distance[29]. In addition, it is suggested that miRNAs may also participate in the regulation of transcription or splicing of transcripts within the nucleus[5,6,27,28].

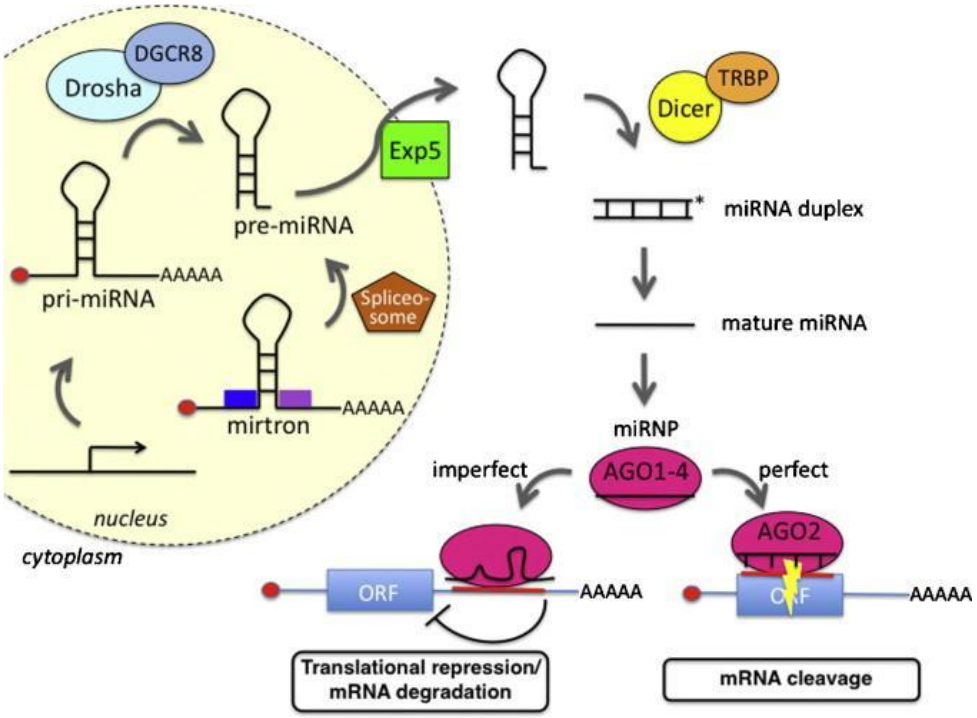

Figure 4 – Schematic representation of the miRNA biosynthesis. Adapted from Breving K, Esquela-Kerscher A. The complexities of microRNA regulation: mirandering around the rules. *Int J Biochem Cell Biol* 2010; 42(8): 1316-1329.

The deregulation of a single miRNA affects the expression of many different proteins and other miRNAs and may lead to several diseases such as vascular diseases and cancer[30].

2. miRNA nomenclature

With the exception of let family of miRNAs, because this was the first family to be discovered, miRNAs are uniformly named using a three-letter abbreviation of the specie they belong to (e.g. hsa is the abbreviation for *Homo sapiens* as mmu is the abbreviation for *Mus musculus*). This prefix is separated by a hyphen from the word

"miR", which is also separated by a hyphen from the corresponding number or number and letter of the miRNA (e.g. hsa-miR-21)[31].

To distinguish both strands of the miRNA duplex, there are two different naming conventions. Accordingly to the relative abundance of the miRNA in the cell, the less abundant form name is followed by a star (e.g. hsa-miR-21*), in opposition to the most abundant one. However, since the relative abundance is not always well known, currently there's a new miRNA labeling depending on the relative position of the mature sequence, considering the pre-miRNA as a reference. In this way, the miRNA with origin in the 5' end of the pre-miRNA gains the suffix "5p" (e.g. hsa-miR-21-5p), whereas the one derived from the 3' end gets the suffix "3p" (e.g. hsa-miR-21-3p). Both classifications are not related once relative abundance of a miRNA is not related to its relative origin position in the precursor[31].

3. Prediction of miRNA putative targets

Unlike plant microRNAs, wherein the complementarity with their targets must be nearly perfect both in coding sequences as in untranslated regions (UTR)[32], most animal microRNAs are more tolerant to imperfect pairing, like G:U pairing, bulged nucleotides and/or mismatches between microRNA and its target[33]. Besides, while plant microRNA targets have only a single binding site, the animal ones have multiple binding sites[34].

For microRNA to bind the target mRNA, it must contain mandatorily a 5'-end seed sequence, the 5'-end segment of the microRNA with 6-8 nucleotides in length, conserved and often flanked by adenosines. Moreover, if there is insufficient base-pairing of this seed, 3'-end of microRNA might support it. The free energy of microRNA:mRNA duplex (ΔG), which is the required energy for the formation of the duplex, and the site accessibility (ΔΔG), which balances the required energy to unfold and to refold of the duplex, are also important for the microRNA:mRNA binding. Besides, the existence of multiple binding sites within a gene for a single microRNA or for different microRNAs allows a dose-dependent and synergistic effect on target expression. Likewise, the sequences around the microRNA binding site like an enrichment of adenosines and uracils, called ALU sequences, may affect the accessibility[35].

Therefore, to predict animal microRNA targets, a computer algorithm is created after the training-set for common distinctive properties like structural and sequence

features of a subset of known microRNAs. This algorithm scores sequences on their similarity to these properties and consequently on their probability to be valid. It is the different weighting and combination of multiple properties that give rise to several algorithms to a more required accuracy[32].

Currently, there are several algorithms that predict microRNA targets, being PicTar, miRanda, TargetScan and TargetScanT the most used ones. However, miRanda and PITA are considered the more accurate databases. To obtain more robust and confident target predictions, there are target prediction portals like miRecords, miRWalk and mirDIP (microRNA Data Integration Portal), which compile several algorithms (Figure 5)[32].

miRecords is a very complete portal allowing the combination of till 11 algorithms (DIANA-microT, MicroInspector, miRanda, miRDB, miRTarget2, miTarget, NBmiRTar, PicTar, PITA, RNA22, RNAhybrid and TargetScan) and it permits the restriction to present the prediction of at least a desired number of databases, not selecting them neither putting bias[36].

miRWalk provides information of microRNA-target interactions from human, mouse and rat by 8 programs (RNA22, miRanda, miRDB, TargetScan, RNAhybrid, PITA, PICTAR and Diana-microT) and it is applied not only to the 3'UTR, but to the whole sequence (promoter, 5'UTR, CDS, 3'UTR). This portal allows the selection of the desired prediction programs[37].

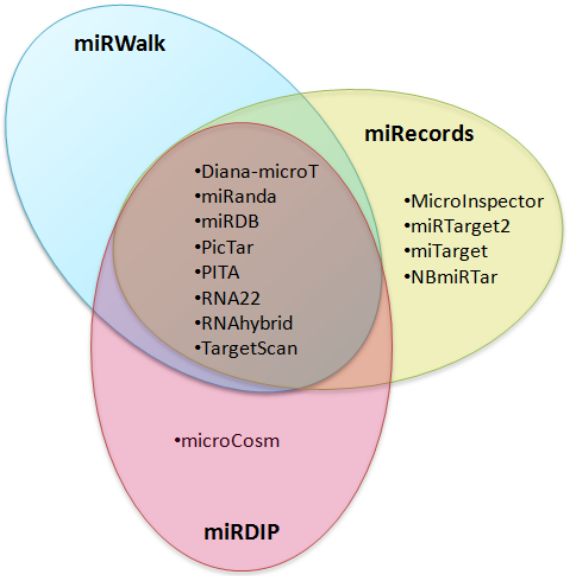

Figure 5 - Schematic representation of miRNA multiple target prediction portals.

mirDIP is an up-to-date portal that also integrates several prediction algorithms. Each algorithm takes into account the characteristics of microRNA:mRNA target interaction in different proportions, allowing the researcher to manage combinations of databases and database characteristics options[35].

MicroRNA-21

In *Homo sapiens*, miR-21 is mapped on chromosome 17q23.2 in an intronic region within a gene, TMEM49, which encodes a human transmembrane protein involved in cell-to-cell adhesion, homolog of rat vacuole membrane protein (VMP1). In mouse, it is expressed in chromosome 11. Despite this, miR-21 has its own promoter regions, being independently regulated[8,38].

This miRNA belongs to the typical miRNA signature of the vasculature and is selectively regulated by several conserved enhancer molecules such as the activation protein 1 (AP-1) that is composed of Fos and Jun family nuclear oncogenes, Ets/PU.1, CCAAT enhancer binding protein α (C/EBP-α), nuclear factor I (NFI), serum response factor (SRF), p53 and signal transducer and activator of transcription 3 (STAT3)[6,38]. MiR-21 and NFIB have a double-negative feedback, which supports miR-21 expression.

Besides, some tumor suppressor elements like forkhead box O3 (Foxo3a) and BMP-6 may negatively regulate miR-21, while tumor growth factor β (TGFβ) appears to upregulate its expression[8,39,40].

This miRNA has likewise numerous targets[41]. However, very few pathways are known to be triggered by miR-21. However, it is consensual that its overexpression suppresses PTEN expression, which leads to an increase in hypoxia inducible factor (HIF)-1α and VEGF levels (not HIF-1β because it is constitutively active) through AKT and extracellular signal-regulated kinase (ERK)1/2 pathway and consequently promotes angiogenesis[7].

MiR-21 is then described to act as a tumor promoter, a genuine oncomiR, in almost every classes of human cancers[41]. This includes breast cancer, glioma, retinoblastoma, colangiocarcinoma, colorectal cancer, renal carcinoma, hepatocellular carcinoma, non-small cell lung cancer (NSCLC) and hematological malignancies such as chronic lymphatic leukemia, acute myeloid leukemia, B-cell lymphoma and Hodgkin's lymphoma[8,42,43,44,45].

Most of tumors with miR-21 upregulated have STAT3 constitutively and inappropriately activated. For instance, in Sézary Syndrome, a rare leukemic cutaneous T-cell lymphoma (CTCL), STAT3 is upregulated through IL-21 stimulation of CD4+ T cells. As a result, STAT3 is constitutively active in these cells and directly targets miR-21. So, expression of miR-21 is increased in neoplastic CD4+ cells from Sézary patients[38]. However, STAT3 seems to have a paradoxical role as its activation through interferon β (IFNβ) regulates miR-21 expression in a negative way. This paradox may be explained by the context, different stimuli and cell types[8].

Besides being expressed in neoplastic and hypoxic conditions, under normal physiological conditions, miR-21 is usually expressed in post-mitotic basal and suprabasal layers of the epidermis[46] as well as in hair follicle epithelium in mouse skin, but it was not seen in the dermis[47]. Its expression might also be found in the liver, being upregulated during the proliferative phase of liver regeneration[48] and in the placenta[49]. In addition, miR-21 is highly induced by luteinizing hormone (LH) in murine granulosa cells[50]. Furthermore, it is transiently upregulated during the differentiation of the human adipose-derived stem cells (hASCs), modulating TGFβR2 expression, which suggests that miR-21 controls adipocyte differentiation[51]. MiR-21 is also present in the heart of mice[52], being in high levels in cardiac fibroblasts[53]. However, normal brain seems to have low levels of it[53]. It is expressed in mouse motor neuron MN-1 cells as well[55,56].

The physiological high expression levels of miR-21 in primary bone marrow–derived monocyte/macrophage precursors (BMMs) are mandatory for osteoclastogenesis, process stimulated by the receptor activator of nuclear factor κB ligand (RANKL). These high levels of miR-21 may also be required for myeloid differentiation. Nevertheless, although it is described that miR-21 is promonopoietic, given that it increases monocytic cell number[57], the role of miR-21 in normal myelopoiesis remains to be clarifyed[58]. In the bone marrow, it is only known that miR-21 is one of the most abundant miRNA expressed in all T cell subsets, being involved in *in vivo* differentiation of human CD8+ T lymphocytes[59]. Even so, its function in the bone marrow microenvironment, and in particular in the bone marrow endothelial cells is still unknown.

Given the lack of information on the function of miR-21 in angiogenesis or in angiocrine factors function, it is legitimate to speculate that miR-21 may potentially be exploited for therapeutic purposes such as for the treatment of bone metabolic disorders with excessive osteoclast development and activity, such as osteoporosis,

and for the treatment of proliferative vascular diseases, such as atherosclerosis and stroke. MiR-21 targeting therapy has great clinical usage potential independent of PTEN status[44].

Aims

In this project, it was proposed to evaluate the role of miR-21 in the bone marrow microenvironment, focusing on bone marrow endothelial cells.

For that purpose, the aims of this work are:

1. Evaluate miR-21 expression on bone marrow cells;
2. Identify predicted targets underlying miR-21 regulation of angiogenesis;
3. Assess endothelial cell phenotypic changes modulated by miR-21 levels;
4. Mice genotyping for further in vivo assays on the miR-21 function.

Methods

Cell Culture

Human umbilical vein endothelial cells (HUVECs) were used for transfection experiments in the fourth passage. Cells were cultured in endothelial cell basal medium-2 (EBM-2), from Lonza, supplemented with hydrocortisone, human fibroblast growth factor (hFGF), VEGF, a recombinant analog of human insulin-like growth factor-1 (R3-IGF-1), ascorbic acid, human epidermal growth factor (hEGF), heparin, gentamicin, amphotericin and containing 10% fetal bovine serum (FBS) in a flask coated with 0,2% gelatin. They were incubated at 37ºC with 5-10% CO_2 supplied and 100% relative humidity, free of contamination.

HUVECs Transfection

HUVECs transfection was done using an Ambion® Anti-miR™ miRNA inhibitor (anti-miR-21) or an Ambion® Pre-miR™ miRNA precursor (pre-miR-21) or an Ambion® negative control, the scramble (Sc), all in a final concentration of 5 µM. Anti-miRs® are single-stranded, synthetic miRNA inhibitors which bind specifically and inhibit the activity of endogenous miRNA. Pre-miRs®, on the other hand, are double-stranded molecules whose function in cell is similar to that of endogenous miRNAs. Scramble has the same nucleotide composition, but not the same sequence and serves as a negative control of transfection, which distinguishes sequence-specific silencing from non-specific effects. Triplicates were performed for each condition.

Electroporation cuvettes (BioRad®) were sterilized through ultraviolet radiation in a laminar air flow chamber for at least 15 minutes. In addition, 6-well plate, previously covered with 0,2% gelatin, was prepared with EBM-2 with 10% FBS, supplements, but without antibiotics.

HUVECs, maintained in log phase growth at 50-80% confluency, were washed twice with Dulbecco's phosphate-buffered saline (DPBS®), from Invitrogen, to remove cellular waste. After that, an incubation with a solution of trypsin 1x at 37ºC for around 2 minutes detached cells from the flask surface. Cells were then homogenized in Dulbecco's modified eagle medium (DMEM®), from Invitrogen, with 10% FBS, which

inhibits the action of trypsin, and were counted on a Neubauer improved hemocytometer. $3x10^5$ cells/well were collected and centrifuged at 1200 rpm during 5 minutes. Discarded the supernatant, the pellet was resuspended in 500µl/well of Opti-MEM® (Invitrogen) without FBS and without antibiotics, whereof 500 µl were distributed to each cuvette. Then, 5 µM of the modulator were added to each condition and each mix was finally electroporated by the Gene Pulser Xcell™ Electroporation System, with 1 pulse of 220 Volts (V), with a capacitance of 500 microfaradays (µF) and a cuvette gap of 4 milimeters (mm). Transfected HUVECs were immediately transferred to the respective well in the previously prepared plate and were incubated at 37ºC with 5% CO_2 for 48 hours for the transfection to take place.

RNA Extraction

High-quality total RNA was purified through TRIzol® method, also known as guanidine isothiocyanate method. TRIzol® Reagent (Sigma-Aldrich) is a monophasic solution of phenol and guanidine isothiocyanate which lyses cells and prevents the activity of RNase enzymes, by denaturing them.

After homogenization of the samples with this reagent, chilled chloroform (200µl/ml TRIzol® Reagent) was added. Samples were homogenized once again and centrifuged at 14000 rpm during 20 minutes at 4ºC for the phase separation to occur. At this point, 3 phases are visible: a red organic phase, which contains protein, a white interphase containing DNA and a colorless upper aqueous, where RNA remains exclusively. Afterward, for the RNA precipitation, this upper aqueous phase was carefully transferred into a fresh tube, mixed with chilled isopropanol (500µl/ml TRIzol® Reagent) and kept O/N at -20ºC. A new centrifugation at 14000 rpm during 20 minutes at 4ºC formed a pellet on the side and bottom of the tube. Supernatant was discarded and RNA pellet was washed twice with chilled 80% ethanol in diethylpyrocarbonate (DEPC)-treated water (1ml/ml TRIzol® Reagent), through vortexing followed by centrifugation at 14000 rpm during 20 minutes at 4ºC. Finally, briefly dried RNA pellet was resuspended in DEPC-treated water and RNA concentration was measured on a NanoDrop® 1000 Spectrophotometer (Thermo Fisher Scientific), which measures 1 µl samples with high accuracy. RNA was always stored at -80ºC.

cDNA Synthesis

1. cDNA Synthesis for analysis of miRNA levels

cDNA for analysis of miRNA levels was synthesized from 500 ng of total RNA using the NCode™ miRNA First-Strand cDNA Synthesis Kit (Invitrogen). This method provides the polyadenylation of mature miRNAs from total RNA and synthesis of cDNA from the tailed miRNAs for use in real-time quantitative polymerase chain reaction (RT-qPCR).

First, 10 mM ATP was diluted in 1 mM Tris (pH 8.0) in a 1:4 proportion. The addition of poly(A) tails to the total RNA was achieved through the incubation of 500 ng/µl of total RNA with the master mix 1, during 15 minutes at 37ºC in a thermal cycler.

Master mix 1	**1X**
5X miRNA Reaction Buffer	5 µl
25 mM $MnCl_2$	2,5 µl
10 mM ATP (diluted 1:4)	1 µl
Poly A Polymerase	0,5 µl
DEPC-treated water	Up to the final volume (23 µl)

After that, 6 µl of the polyadenylated template was taken to continue the cDNA synthesis, while the remaining was stored at -80ºC. Master mix 2 was added to the 6 µl polyadenylated RNA, incubated at 65ºC during 5 minutes and placed 1 minute on ice. Then, polyadenylated RNA was reverse transcribed through the addition of master mix 3 and incubation at 50 ºC for 50 minutes followed by 85 ºC for an additional 5 minutes, in order to stop the reaction. cDNA samples were stored at -20ºC.

Master mix 2	**1X**
Annealing Buffer	1 µl
Universal RT Primer (25 µl)	3 µl

Master mix 3	**1X**
2X First-Strand Reaction Mix	10 µl
SuperScript® III RT/ RNaseOUT® Enzyme Mix	2 µl

2. cDNA Synthesis for analysis of expression of coding genes

To analyze the expression of coding genes, cDNA was synthesized from 500 ng of total RNA, to which was added the master mix 1. It was incubated 5 minutes at 65ºC and then added the master mix 2, previously incubated 2 minutes at 25ºC.

Master mix 1	**1X**
2,5 µM dNTPs	1 µl
Random Primers	1 µl

Master mix 2	**1X**
5X First Strand Buffer	4 µl
0,1 M DTT	2 µl
RNase-OUT	1 µl

Finally, 1 µl of SuperScript® II RT enzyme was added to each tube, followed by incubations of 10 minutes at 25ºC, 50 minutes at 42ºC and 15 minutes at 70ºC. cDNA products were diluted in DEPC-treated water, in the proportion of 1:2, and stored at -20ºC.

Real-time Quantitative PCR (RT-qPCR)

The amplification and relative quantification of coding and non-coding genes (miRNAs) was performed in a ViiA™ 7 Real-Time PCR System (Applied Biosystems®) instrument in 384-well plates. Relative quantification was carried out through the comparative threshold cycle (Ct) method (ΔΔCt).

The run method was started with the hold stage (2 minutes at 50ºC and 10 minutes at 95ºC), then 40 cycles of 15 seconds at 95ºC and 1 minute at 60ºC were used for the PCR stage, and finally the melt curve stage with 15 seconds at 95ºC and 1 minute at 60ºC.

1. Quantification of miRNA levels

To perform RT-qPCR for the analysis of miRNA levels, the Power SYBR® Green PCR Master Mix and the Universal qPCR Primer (Applied Biosystems®) were used. The other primer used in the reaction was the sequence of the miRNA to be analyzed. In the case of hsa-miR-21-5p, it was: 5'-TAGCTTATCAGACTGATGTTGA-3'. However, human U6 and 18S, the housekeeping genes used for the normalization, have their own specific forward and reverse primers.

Primer	Sequence 5' - 3'
U6 Forward	GTGCCGCTTCGGCAGCACATATAC
U6 Reverse	AAAAATATGGAACGCTTCACGAATTTG
18S Forward	GCCCTATCAACTTTCGATGGTAGT
18S Reverse	CCGGAATCGAACCCTGATT

The following master mix were distributed per well of the 384-well plate with 2 µl of cDNA. The plate was carefully sealed and centrifuged at 1400 rpm during 2 minutes at 4ºC.

Master mix	1X
Bidistilled water	2,6 µl
SYBR® Green PCR Master Mix	3,5 µl
2% Bovine serum albumin (BSA)	0,075 µl
10 µM UniPrimer qPCR	0,15 µl
10 µM hsa-miR-21-5p Primer	0,15 µl

2. Quantification of coding genes

Also to perform the RT-qPCR for analysis of the expression of coding genes, Power SYBR® Green PCR Master Mix was used. Though, each gene has its own specific forward and reverse primers and only human 18S was used as housekeeping gene.

Primer	Sequence 5’ - 3’
18S Forward	GCCCTATCAACTTTCGATGGTAGT
18S Reverse	CCGGAATCGAACCCTGATT
Jagged1 Forward	CGGCTTTGCCATGTGCTT
Jagged1 Reverse	TCTTCCTCCATCCCTCTGTCA
PTEN Forward	TGTTGTTTCACAAGATGATGTTTGA
PTEN Reverse	CAGACCACAAACTGAGGATTG
RhoB Forward	ATGTGCTTCTCGGTGGACAG
RhoB Reverse	GATGGGCACATTGGGACAGA
RECK Forward	CAGGTCTGCCTGACGACTTT
RECK Reverse	GCTCCATGTGGTCTGTGTCA
Annexin A1 Forward	AACAGGAAAGCCCCTGGATG
Annexin A1 Reverse	TGGCAGCACGAAGTTCATCA
IL-15 Forward	ACAGAAGCCAACTGGGTGAA
IL-15 Reverse	TGCAACTGGGGTGAACATCA
Spry1 Forward	GGAAATCCACGGTGATCCT
Spry1 Reverse	GGCATGCATCTGAAATCCTT
Spry2 Forward	TCAGAGCCATCCGAAACACC
Spry2 Reverse	TCGTGTTTGTGCTGAGTGGA
TSP-1 Forward	TGGAGCGGAAAGACCACTCT
TSP-1 Reverse	CCGCCTTGCCATTGGA

The following master mix were distributed per well of the 384-well plate with 2 µl of cDNA. The plate was carefully sealed and centrifuged at 1400 rpm during 2 minutes at 4ºC.

Master mix	1X
Bidistilled water	2 µl
SYBR® Green PCR Master Mix	4 µl
10 µM UniPrimer qPCR	0,15 µl
10 µM hsa-miR-21-5p Primer	0,15 µl

Matrigel Assay

BD Matrigel™ Basement Membrane Matrix Growth Factor Reduced was used to perform tube formation assay. It is composed by a mixture of basement membrane components, which stimulates endothelial cells to attach and differentiate.

To each well of a 24-well plate was added 5 unid/ml heparin to be dissolved with 200 ml of BD Matrigel™ Basement Membrane Matrix Growth Factor Reduced. In addition, 50 ng/ml VEGF and 5 ng/ml bFGF were added to the respective condition, to be tested individually. Then $3x10^5$ transfected HUVECs were added to each well and 24 hours later, tube formation was measured counting the number of tubules formed.

"Wound healing/Scratch" Assay

After the transfection of cells in a 0,2% gelatin coated plate, cells were left to grow until confluence was achieved. With the help of a 10 µl tip, a simple scratch of the cell monolayer was carefully performed not to detach gelatin. Pictures were taken at the time points 0, 6, 12 and 24 hours and migration was evaluated through the measurement of the size of the "wound", a measure of the rate of cell migration in response to the different experimental conditions.

Mice Genotyping

Mice were genotyped by PCR. Each mouse was labeled and 0,5 cm of the tail was cut into an Eppendorf tube. This tail tip was then digested in 300 µl Laird's buffer and 3 µl proteinase k at 55ºC O/N with shaking. After spinning down the hairs and bones, supernatant was collected to a fresh tube and DNA was precipitated with 300 µl isopropanol, by just inverting the tube. DNA was then fished into 200 µl bidistilled water and dissolved at 37ºC with shaking for 1 hour. 2 µl of this DNA solution was used to perform the followed PCR reactions.

Master mix for VE-Cadh-Cre-ER^{T2}	**1X**
10X PCR buffer	2,5 µl
10 mM dNTPs	0,5 µl
40 mM $MgCl_2$	2 µl
10 µM Cre 313U	0,7 µl
10 µM Cre 6831	0,7 µl
Bidistilled water	16,3 µl
Taq polymerase	0,3 µl

Master mix for miR-21^{lox}	**1X**
10X PCR buffer	2,5 µl
10 mM dNTPs	0,5 µl
40 mM $MgCl_2$	2 µl
10 µM miR-21 conditional Fwd	0,7 µl
10 µM miR-21 conditional Rev	0,7 µl
Bidistilled water	16,3 µl
Taq polymerase	0,3 µl

Master mix for Dll4^{lox}	**1X**
10X PCR buffer	2,5 µl
10 mM dNTPs	0,5 µl
40 mM $MgCl_2$	1 µl
10 µM Dll4 lox 5’	0,7 µl
10 µM Dll4 lox 3’	0,7 µl
Bidistilled water	17,3 µl
Taq polymerase	0,3 µl

These reactions took place in the thermal cycle with the following PCR program: 1 cycle at 95ºC during 3 minutes, 35 cycles of 30 seconds at 95ºC, 30 seconds at 60ºC and 35 seconds at 72ºC, and a final cycle at 72ºC during 3 minutes.

The primer sequences used are listed above.

Primer	Sequence 5’ – 3’
Cre 313U	CCAGCTAAACATGCTTCATC
Cre 6831	CGCTCGACCAGTTTAGTTAC
miR-21 conditional 5’	GCTTACTTCTCTCTGTGATTTCTGTG
miR-21 conditional 3’	GGTGGTACAGCCATGCGATGTCACGAC
Dll4 lox 5’	GTGCTGGGACTGTAGCCACT
Dll4 lox 3’	TGTTAGGGATGTCGCTCTCC

Solutions:

Laird’s buffer	
1 M Tris-HCl pH 8,5	50 ml
0,5 mM EDTA	5 ml
20% SDS	5 ml
5 mM NaCl	20 ml
Ultrapure water	Till 500 ml

Lysis buffer	
3 M KCl	834 µl
1 M Tris-HCl pH 8,3	500 µl
1 M $MgCl_2$	100 µl
10% Tween 20	2,25 ml
10% NP40	2,25 ml
Ultrapure water	Till 50 ml

After amplification, DNA samples were run in a 2% (w/v) agarose gel in tris-borate-EDTA (TBE) 0,5X. For DNA to be visible under UV light, 2,5% GelSafe or 4% Ethidium Bromide (EtBr) were added to the gel. Electrophoresis was carried out with 5 µl molecular weight marker 50 bp ladder (Invitrogen) as a ruler and bands were seen through a UV transilluminator.

Statistical Analysis

Statistical significant differences were defined as $p<0,05$ and were calculated by unpaired two-tailed Student’s t test. Data were expressed as mean ± standard deviation of the mean. Statistical analysis and graphs were achieved using GraphPad® Prism 5.0 software.

Results and Discussion

miR-21 expression on bone marrow cells

In order to evaluate the levels of expression of miR-21 in hematopoietic stem cells (HSCs), endothelial cells (Lin^- VE-$Cadh^+$) and other hematopoietic (committed) cells (Lin^+) isolated from mouse bone marrow, a RT-qPCR was performed. The Lineage Antibody Cocktail (Lin), as the name suggests, is a cocktail of antibodies that recognize mature cells markers. Therefore, lineage-negative (Lin^-) cells are not committed yet. VE-Cadherin (VE-Cadh) is an endothelial specific marker, hence only VE-$Cadh^+$ cells are considered endothelial.

As observed in Figure 6, committed cells in general (Lin^+) and endothelial cells (Lin^- VE-$Cadh^+$) express significantly more miR-21 than HSCs.

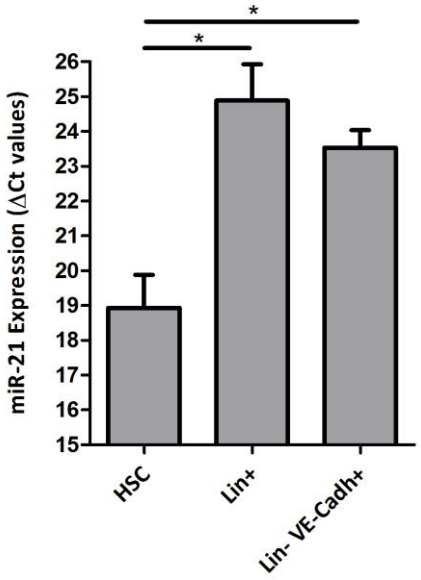

Figure 6 - miR-21 expression in bone marrow subpopulations measured by RT-qPCR. Error bars represent standard deviation (SD).

hsa-miR-21-5p predicted targets

The identification of miRNA predicted targets transcripts is reached through experiments, through the matching of sequences and through sites-specific mutagenesis or other techniques.

In order to investigate the downstream targets underlying miR-21 regulation of angiogenesis, a bioinformatic approach was used besides the literature.

A research in the European Bioinformatics Institute site (http://www.ebi.ac.uk/enright-srv/microcosm/htdocs/targets/v5/) with the gene EnsEMBL identifier (http://www.ensembl.org/index.html) was very useful in the selection of the possible miR-21 predicted target genes. This approach gets the miRNA sequences from the miRBase Sequence Database (http://www.mirbase.org/) and the majority of the genomic sequences from the EnsEMBL and applies the miRanda algorithm. It uses a dynamic programming alignment to identify highly complementary sites which are scored between 0 and 100, where 0 represents no complementarity and 100 complete complementary. It also takes advantage of the Vienna RNA folding package to predict and compare RNA secondary structures, assessing the energy, which is a measure for the thermodynamic stability of the double-stranded anti-parallel duplex.

This evaluation was carried out for angiocrine and angiogenic factors predicted to be miR-21 targets.

1. Angiocrine factors

Butler JM *et al.* have observed that the endothelium may act as a tissue capable of releasing growth factors and/or cytokines, which may act in a paracrine manner on neighboring cells. These factors have been referred as angiocrine factors and may comprise secreted factors as well as membrane-bound molecules or membrane proteins that can give rise to secreted variants[21].

Between all these angiocrine factors (Table 1), only Jagged1 (Jag1) is predicted to match with miR-21 (Table 2).

Jag1 is a key Notch ligand that is important for a variety of cell fate decisions and many cellular biological processes, like the vascularization. It is a potent proangiogenic regulator[60]. Jag1 is expressed in many tissues, predominantly on the surface of

Table 1 – Angiocrine factors: function and organ specificity. Adapted from Butler JM, Kobayashi H, Rafii S. Instructive role of the vascular niche in promoting tumour growth and tissue repair by angiocrine factors. *Nat Rev Cancer* 2010; 10(2): 138-146.

Angiocrine factors produced by the vascular niche

Angiocrine factors	Function	Organ specificity	Refs
BMP2 and BMP4	Organogenesis and tumorigenesis	Nonspecific	66
FGF2	Organogenesis and tumorigenesis	Nonspecific	4
BDNF	Neurogenesis	Brain and heart	68
PEDF	Neurogenesis	Brain and bone marrow	67
PGF	Angiogenesis and tumorigenesis	Nonspecific	117
PDGFβ	Angiogenesis and tumorigenesis	Smooth muscle	60,86,118
VEGFA	Angiogenesis and autocrine loop	Vasculature	119
ANGPT2	Angiogenesis remodelling	Vasculature	26
Jagged 1 and jagged 2	Haematopoiesis, angiogenesis and tumorigenesis	Bone marrow	83,110
LAMA4	Organogenesis and tumorigenesis	Stem cell niches	11,62
NO	Tumorigenesis and leukaemogenesis	Nonspecific	76
IL-8, IL-6, CD40, G-CSF, GM-CSF, IGF1, SDF1, EDN1, MCP1 and TGFβ	Tumorigenesis and tissue repair	Nonspecific	60,106

ANGPT2, angiopoietin 2; BDNF, brain-derived nerve growth factor; BMP, bone morphogenetic protein; CSF, colony stimulating factor; EDN1, endothelin 1; FGF, fibroblast growth factor; G-CSF, granulocyte-CSF; GM-CSF, granulocyte-macrophage-CSF; IGF, insulin-like growth factor; IL, interleukin; LAMA4, laminin α4; MCP1, monocyte chemotactic protein 1 (also known as CCL2); NO, nitric oxide; PDGFβ, platelet-derived growth factor-β; PEDF, pigmented epithelial growth factor; PGF, placental growth factor; SDF1, stromal cell-derived factor 1 (also known as CXCL2); TGFβ, transforming growth factor-β; VEGF, vascular endothelial growth factor.

vascular endothelial cells, acting on Notch receptor in the neighboring vascular smooth muscle cells, following the "canonical" Notch pathway and thus promoting its differentiation and maturation through cell-cell interaction or trans-interaction[61]. In contrast, the same interaction within the same cell (cis-interaction) is thought to inhibit Notch signaling. This angiocrine factor is also involved in the formation of adult hematopoietic stem cells from the aorta[61].

Table 2 - Alignment of the Jag1 3'UTR with the miR-21 sequence, through MicroCosm Targets. It provides the Ensembl gene accession, binding score, miRNA binding site, nucleotide starting and end of the mRNA binding site.

Gene Name	JAG1								
Transcript	ENST00000254958								
Gene	ENSG00000101384								
Description	Jagged-1 precursor (Jagged1) (hJ1) (CD339 antigen). [Source:Uniprot/SWISSPROT;Acc:P78504]								
Hit infomation	Rfam ID	Score	Energy	Base P	Poisson P	Org P	Start	End	Alignment
	hsa-miR-21	15.7297	-12.23	5.121250e-02	4.992320e-02	4.221070e-05	1220	1241	AGUUGUAGUCAGACUAUUCGAU | :: | :| ||| ||||||| TAGGGAGTATTCTAATAAGCTA

The 3'UTR of Jag1 is a functional target of miR-21, which triggers its translational suppression[62,63]. The importance of this interaction is confirmed by Selcuklu SD *et al.* 2012, whose results indicate that 17beta-estradiol (E2) enhances Jag1 expression, in ER^+ breast cancer cells, by reducing the levels of miR-21[63].

2. Angiogenic factors

The angiogenic factors are molecules that stimulate the growth of new blood vessels by modulating endothelial cell properties including proliferation, survival, migration, invasion, among others. Annexin A1 (ANXA1) (Table 3), interleukin (IL)-15 (Table 4), PTEN, reversion-inducing cysteine-rich protein with Kazal motifs (RECK), Ras homolog gene family, member B (RhoB), Sprouty1 (Spry1) (Table 5Table 5), Sprouty2 (Spry2) (Table 6) and thrombospondin1 (TSP-1) (Table 7) are predicted to be targets of miR-21 either by bioinformatic tools and/or by literature.

2.1. ANXA1

Annexin A1 (ANXA1) is a calcium-dependent phospholipid binding protein that is found in several tissues like lung, bone marrow and intestine. It is involved in many biological processes such as anti-inflammatory signalling, maintenance of cytoskeleton and ECM integrity, tissue growth, apoptosis and differentiation[64]. The activation of the p38/MAPKAP kinase-2/LIMK1/ANXA1 signaling axis is shown to be implicated in the endothelial cell migration, induced in response to vascular endothelial growth factor (VEGF)[65]. Therefore, ANXA1 is a regulator of this angiogenic effect.

Even though there's no evidence of it in the literature, in silico analysis reveals that ANXA1 contains a miR-21 binding site, which is complementary to the miR-21 seed sequence in the 3' untranslated region (3'-UTR).

Table 3 - Alignment of the ANXA1 3'UTR with the miR-21 sequence, through MicroCosm Targets. It provides the Ensembl gene accession, binding score, miRNA binding site, nucleotide starting and end of the mRNA binding site.

Gene Name	ANXA1								
Transcript	ENST00000257497								
Gene	ENSG00000135046								
Description	Annexin A1 (Annexin I) (Lipocortin I) (Calpactin II) (Chromobindin-9) (p35) (Phospholipase A2 inhibitory protein). [Source:Uniprot/SWISSPROT;Acc:P04083]								
Hit infomation	Rfam ID	Score	Energy	Base P	Poisson P	Org P	Start	End	Alignment
	hsa-miR-21	17.0555	-10.99	1.335060e-02	1.326190e-02	3.487830e-03	47	67	GUUGUAGUCAGACUAUUCGA :| : ||| || |||||| TATTTTCA-TCCTATAAGCT

2.2. IL-15

Interleukin (IL)-15 is expressed mainly by monocytes, fibroblasts, epithelial cells, and stromal cells from bone marrow and thymus. This cytokine is a stimulator of angiogenesis in vivo[66]. It induces T-cell proliferation and chemotaxis, promotes natural killer cell growth, the release of IFN-ɣ, granulocyte/macrophage colony stimulating factor and TNF-α and it co-stimulates B-cell growth and Ig production[67].

Although there is no evidence in the literature, IL-15 seems to include a miR-21 binding site, which is complementary to the miR-21 seed sequence in the 3' untranslated region (3'-UTR).

Table 4 - Alignment of the IL-15 3'UTR with the miR-21 sequence, through MicroCosm Targets. It provides the Ensembl gene accession, binding score, miRNA binding site, nucleotide starting and end of the mRNA binding site.

Gene Name	IL15								
Transcript	ENST00000296545								
Gene	ENSG00000164136								
Description	Interleukin-15 precursor (IL-15). [Source:Uniprot/SWISSPROT;Acc:P40933]								
Hit infomation	Rfam ID	Score	Energy	Base P	Poisson P	Org P	Start	End	Alignment
	hsa-miR-21	15.782	-21	4.859830e-02	4.743630e-02	4.743630e-02	403	425	AGUUGUAG-UCAGACUAUUCGA |||||| | | |||:||:||| TCAACAGCTATGCTGGTAGGCT

2.3. PTEN

Phosphatase and tensin homolog (PTEN) has a tumor suppressor function and is known to be modulated by miR-21 both directly, through sites within its 3'UTR, and indirectly, through inhibition of Sprouty2[68]. Targeting PTEN, miR-21 induces angiogenesis, through AKT and MAPK/ERK1/2 signaling pathways, increasing HIF-1α and VEGF expression[40]. In addition, PTEN controls cell migration and invasion, regulating MMP2 and MMP9, activity inhibited by the action of miR-21[39].

2.4. RECK

It has been described that miR-21 promotes migration and invasion by targeting inhibitors of MMPs, one of which is Reversion-inducing cysteine-rich protein with Kazal motifs (RECK). RECK is a membrane-anchored glycoprotein, very important for normal development, that seems to have the ability to increase vessel formation within a matrix while maintaining vessel wall thickness. Thus, it has an essential role in angiogenesis[69,70].

2.5. RhoB

Ras homolog gene family, member B (RhoB) is involved in intracellular trafficking of several proteins and it supports endothelial cell survival, morphogenesis, migration and angiogenesis. RhoB is described in literature to be a direct target of microRNA-21 in its 3'UTR[71,72,73].

2.6. **Spry1** and **Spry2**

Sprouty (Spry) are membrane-anchored phosphoproteins that inhibit growth factor signaling in endothelial cells[74].

Sprouty1 (Spry1), an intrinsic inhibitor of the Ras/MEK/ERK pathway, was found in vascular endothelial cells and has been shown to inhibit vasculogenesis[75]. It also has an important role in the lineage specific differentiation of mouse embryonic stem cells (mESCs)[76]. Spry1 was found to be a miR-21 target in cardiac fibroblasts[77].

Table 5 - Alignment of the Spry1 3'UTR with the miR-21 sequence, through MicroCosm Targets. It provides the Ensembl gene accession, binding score, miRNA binding site, nucleotide starting and end of the mRNA binding site.

Gene Name	SPRY1								
Transcript	ENST00000339241								
Gene	ENSG00000164056								
Description	Sprouty homolog 1 (Spry-1). [Source:Uniprot/SWISSPROT;Acc:O43609]								
Hit infomation	Rfam ID	Score	Energy	Base P	Poisson P	Org P	Start	End	Alignment
	hsa-miR-21	15.4735	-8.88	6.613570e-02	6.399620e-02	8.139270e-04	401	422	aguugUAGUCAGACUAUUCGAU ||:: |: |||||||| gtttaATTGCTTAAATAAGCTA

MiR-21 is shown to directly target Sprouty2 (Spry2) in cardiocytes, promoting their proliferation and migration[78]. In addition, by repressing Spry2, this particular microRNA has a critical influence in the duration and magnitude of ERK-MAPK activity, being described to enhance the MSCs differentiation during osteogenesis[79].

Table 6 - Alignment of the Spry2 3'UTR with the miR-21 sequence, through MicroCosm Targets. It provides the Ensembl gene accession, binding score, miRNA binding site, nucleotide starting and end of the mRNA binding site.

Gene Name	SPRY2								
Transcript	ENST00000377104								
Gene	ENSG00000136158								
Description	Sprouty homolog 2 (Spry-2). [Source:Uniprot/SWISSPROT;Acc:O43597]								
Hit infomation	Rfam ID	Score	Energy	Base P	Poisson P	Org P	Start	End	Alignment
	hsa-miR-21	15.6224	-12.12	5.701740e-02	5.542240e-02	4.753090e-03	222	243	aguuGUAGUCAGACUAUUCGAU ||| |: |||||||| gaccCATGTATTGCATAAGCTA

2.7. TSP-1

Thrombospondin1 (TSP-1) is an ECM glycoprotein that inhibits angiogenesis naturally and acts like a tumor suppressor, activating the TGF-β signaling pathway[80].

Even though there is no evidence in the literature, in silico analysis reveals that TSP-1 contains a miR-21 binding site, which is complementary to the miR-21 seed sequence in the 3' untranslated region (3'-UTR).

Table 7 - Alignment of the TSP-1 3'UTR with the miR-21 sequence, through MicroCosm Targets. It provides the Ensembl gene accession, binding score, miRNA binding site, nucleotide starting and end of the mRNA binding site.

Gene Name	THBS1								
Transcript	ENST00000260356								
Gene	ENSG00000137801								
Description	Thrombospondin-1 precursor. [Source:Uniprot/SWISSPROT;Acc:P07996]								
Hit infomation	Rfam ID	Score	Energy	Base P	Poisson P	Org P	Start	End	Alignment
	hsa-miR-21	17.4036	-22.72	9.350550e-03	9.306970e-03	9.306970e-03	1248	1269	ag UUGUAGUCAGACUAUUCGAU || |||||||| |||||||: gg AAAATCAGTCTAATAAGCTG

Nevertheless, some of these predictions were confirmed by miRecords (Table 8) and miRDIP (Table 9), the chosen portals to cover all the applications for miRNA target predictions.

Table 8 - Angiogenesis related predicted targets for hsa-miR-21 through miRecords portal last updated at April 27, 2013. 5 targets were predicted (marked in blue) by at least 5 algorithms. The NCBI accession number is provided as RefSeq for each predicted target.

miRNA	**Target Gene**		**Predictions** ● : Interaction predicted ● : Interaction not predicted ↓ : Sort according to predictions made by this program										
Mature ID	Symbol	RefSeq	DIANA-microT	Micro Inspector	mi Randa	Mir Target2	mi Target	NB miRTar	Pic Tar	PITA	RNA 22	RNA hybrid	TargetScan/ TargetScanS
hsa-miR-21	JAG1	NM_000214	●	●	●	●	●	●	●	●	●	●	●
hsa-miR-21	SPRY1	NM_005841	●	●	●	●	●	●	●	●	●	●	●
hsa-miR-21	SPRY2	NM_005842	●	●	●	●	●	●	●	●	●	●	●
hsa-miR-21	RECK	NM_021111	●	●	●	●	●	●	●	●	●	●	●
hsa-miR-21	RHOB	NM_004040	●	●	●	●	●	●	●	●	●	●	●

Table 9 - Angiogenesis related predicted targets for hsa-miR-21 through miRDIP portal last updated in January, 2012. 6 targets were predicted by at least 4 algorithms. The NCBI accession number is provided as RefSeq for each predicted target. Also the respective database measure of confidence in the prediction (Score (origin)) is provided as well as a standardized score (score (std)), which allows the comparison between databases scores and ranges from 0 (least confident) to 100 (most confident).

Gene Symbol	Links	microRNA	Source	Score (orig)	Score (std)	Rank
JAG1	i2D GC	hsa-mir-21	PITA Top Targets	-0.95	37.05	Bottom Third
JAG1	i2D GC	hsa-mir-21	DIANA-microT	8.22	2.09488	Top Third
JAG1	i2D GC	hsa-mir-21	microRNA.org	75.0	60.31746032	Mid Third
JAG1	i2D GC	hsa-mir-21	microCosm Targets (formerly mirBase)	15.7297	24.4845897	Bottom Third
JAG1	i2D GC	hsa-mir-21	picTar 5-way	7.0	0.7	Bottom Third
JAG1	i2D GC	hsa-mir-21	TargetScan Conserved Targets	-0.385	69.67265317	Top Third
RECK	i2D GC	hsa-mir-21	PITA Top Targets	-7.5	48.82	Top Third
RECK	i2D GC	hsa-mir-21	DIANA-microT	8.22	2.09488	Top Third
RECK	i2D GC	hsa-mir-21	microRNA.org	78.0	65.07936508	Top Third
RECK	i2D GC	hsa-mir-21	microCosm Targets (formerly mirBase)	15.4863	21.81967482	Bottom Third
RECK	i2D GC	hsa-mir-21	TargetScan Conserved Targets	-0.474	81.00878869	Top Third
RHOB	i2D GC	hsa-mir-21	PITA Top Targets	-1.57	38.17	Bottom Third
RHOB	i2D GC	hsa-mir-21	DIANA-microT	3.25	0.652836	Mid Third
RHOB	i2D GC	hsa-mir-21	microRNA.org	66.0	46.03174603	Bottom Third
RHOB	i2D GC	hsa-mir-21	TargetScan Conserved Targets	-0.291	57.69965609	Top Third
SPRY1	i2D GC	hsa-mir-21	PITA Top Targets	-0.55	36.33	Bottom Third
SPRY1	i2D GC	hsa-mir-21	DIANA-microT	7.15	1.78442	Top Third
SPRY1	i2D GC	hsa-mir-21	microCosm Targets (formerly mirBase)	15.4735	21.6795314	Bottom Third
SPRY1	i2D GC	hsa-mir-21	RNA22 Coding Region predictions	-28.9	14.2335756	Top Third
SPRY1	i2D GC	hsa-mir-21	TargetScan Conserved Targets	-0.456	78.71608712	Top Third
SPRY2	i2D GC	hsa-mir-21	PITA Top Targets	-0.64	36.5	Bottom Third
SPRY2	i2D GC	hsa-mir-21	DIANA-microT	8.76	2.25156	Top Third
SPRY2	i2D GC	hsa-mir-21	microRNA.org	64.0	42.85714286	Bottom Third
SPRY2	i2D GC	hsa-mir-21	microCosm Targets (formerly mirBase)	15.6224	23.30979362	Bottom Third
SPRY2	i2D GC	hsa-mir-21	picTar 5-way	29.0	2.9	Bottom Third
SPRY2	i2D GC	hsa-mir-21	TargetScan Conserved Targets	-0.31	60.11972997	Top Third
THBS1	i2D GC	hsa-mir-21	DIANA-microT	2.19	0.345278	Mid Third
THBS1	i2D GC	hsa-mir-21	microRNA.org	89.0	82.53968254	Top Third
THBS1	i2D GC	hsa-mir-21	microCosm Targets (formerly mirBase)	17.4036	42.81162753	Top Third
THBS1	i2D GC	hsa-mir-21	RNA22 3' UTR predictions	-32.799999	26.89654828	Top Third
THBS1	i2D GC	hsa-mir-21	TargetScan Non-Conserved Targets	-0.239	52.77078086	Top Third

miR-21 modulation of its predicted targets

In order to ascertain which of all these predicted targets are really modulated by the levels of miR-21, HUVECs from 3 different healthy individuals were transfected in the fourth passage with an anti-miR-21 inhibitor, a pre-miR-21 precursor and a scramble (Sc). Given the difficulty of isolation and maintenance of bone marrow endothelial cells (BMECs), HUVECs were chosen once these are the endothelial cells most commonly used in in vitro experiments. HUVECs, as primary endothelial cells, tend to lose their primary characteristics and responsiveness to various stimuli beyond the sixth passage.

cDNA was synthesized from the extracted RNA and analyzed by RT-qPCR as described in methods section.

RT-qPCR different approaches

This quantitative assay measures the amount of cDNA during each amplification cycle of the PCR in real time, through the intensity signal of a fluorescent reporter molecule, in this case the Power SYBR® Green PCR master mix. It intercalates between double-stranded DNA (dsDNA), not discriminating dsDNA, including primer dimmers.

ViiA™ 7 Real-Time PCR System software gives Ct (threshold cycle) values, which is the intersection between the amplification curve and a threshold line, being a relative measure of the target concentration. Through the mean of each technique replicate Ct values, it was possible to achieve the ΔCt, normalizing Ct means in relation to the housekeeping genes. In a relative quantification, the analysis of changes in miRNA expression in a given sample relative to another reference sample (in this case the scramble) is preferentially given by ΔΔCt, which compares ΔCt values of the samples with a reference sample. Thus, there are several ways of representing the final results of a RT-qPCR. Some of the used RT-qPCR approaches are ΔCt (Figure 7), $2^{-\Delta Ct}$ (Figure 8), $(2^{-\Delta Ct})/(2^{-\Delta Ct}$ mean of the Sc) (Figure 9) that normalizes all the reference sample (Sc) values to 1, ΔΔCt (Figure 10) and $2^{-\Delta\Delta Ct}$ (Figure 11) that set all the reference sample (Sc) values as 0.

Among the first 3 approaches of the same experiment (ΔCt, $2^{-\Delta Ct}$, $(2^{-\Delta Ct})/(2^{-\Delta Ct}$ mean of the Sc)) that are normalized only in relation to the housekeeping genes, a considerable difference is visible in their analysis, even if there are not significant

differences between the conditions (sc, anti-miR-21 and pre-miR-21). While in ΔCt values representation (Figure 7), anti-miR-21 is reducing the miR-21 levels in the HUVECs and pre-miR-21 is slightly increasing them, $2^{-\Delta Ct}$ (Figure 8) and $(2^{-\Delta Ct})/(2^{-\Delta Ct}$ mean of the Sc) (Figure 9) values representation transmit the very opposite. The same occurs between ΔΔCt (Figure 10) and $2^{-\Delta\Delta Ct}$ (Figure 11). So it can be concluded that exponential function ($Y=2^{-x}$) seems to be masking the results, given that the higher value of X, the smaller value of Y. Therefore, the best approaches are ΔCt and ΔΔCt, once it's the best approximation to the absolute values.

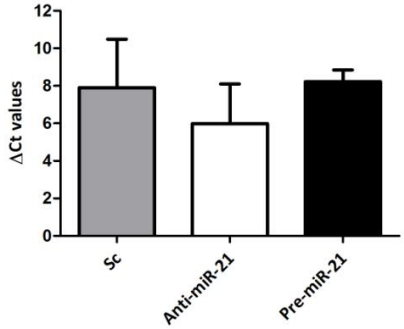

Figure 7 – miR-21 transfection efficiency represented by ΔCt values. Error bars represent standard deviation (SD).

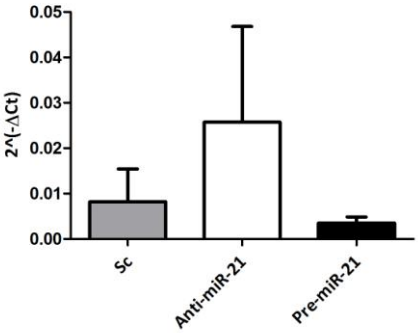

Figure 8 – miR-21 transfection efficiency represented by $2^{-\Delta Ct}$ values. Error bars represent standard deviation (SD).

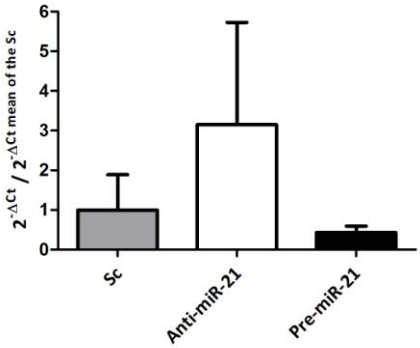

Figure 9 – miR-21 transfection efficiency represented by $\frac{2^{-\Delta Ct}}{2^{-\Delta Ct}\ \text{mean of the Sc}}$ values. Error bars represent standard deviation (SD).

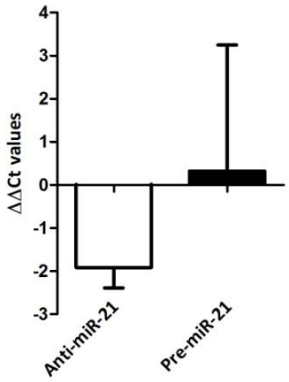

Figure 10 – miR-21 transfection efficiency represented by ΔΔCt values. Error bars represent standard deviation (SD).

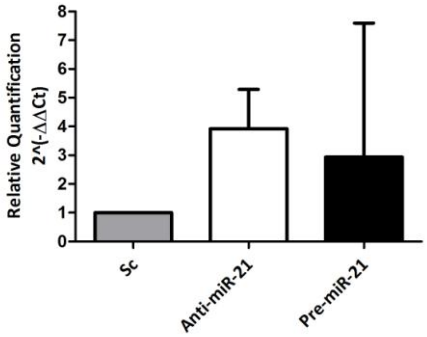

Figure 11 – miR-21 transfection efficiency represented by $2^{-\Delta\Delta Ct}$ values. Error bars represent standard deviation (SD).

Validation of mir-21 predicted targets

The housekeeping genes are crucial for the estimation and comparison of mRNA levels. 18S, a part of ribosomal RNA, is a very abundant and stable housekeeping gene as it has a constant expression level across the samples. U6, in turn, is a small nuclear RNA (snRNA) is a good normalizer for the assessment of miRNA levels. Thus, in order to evaluate the miR-21 transfection efficiency, 18S and U6 were used as housekeeping genes, while in the analysis of the genes expression just 18S was used.

In the first experiment, most probably because of the transfection failure (Figure 12), pre-miR-21 precursor did not work (Figure 13), since all the predicted targets are more expressed in this condition than in the scramble. However, anti-miR-21 inhibitor slightly upregulated the expression of all the studied genes, improving significantly PTEN and RhoB gene expression.

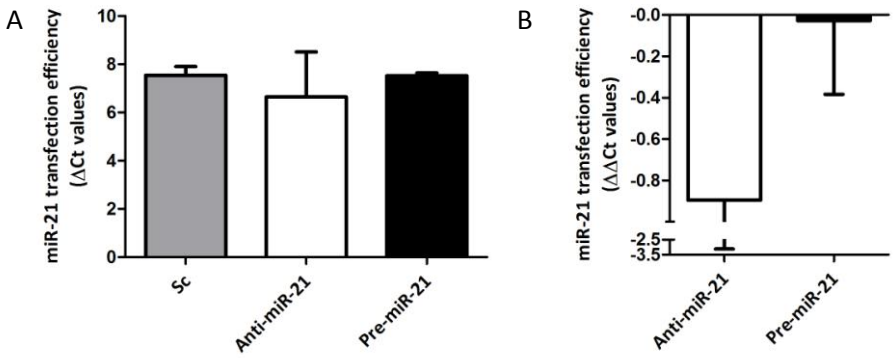

Figure 12 – miR-21 transfection efficiency in the first experiment. A) ΔCt values representation; B) ΔΔCt values representation, where Sc is the baseline (0). Error bars represent standard deviation (SD).

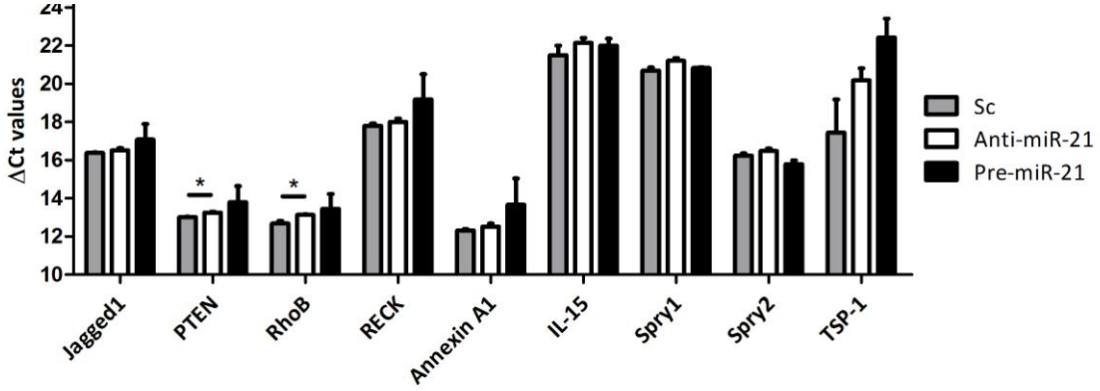

Figure 13 – Gene expression modulated by miR-21 levels for the first experiment. Only PTEN and RhoB were validated by the inhibition of miR-21 expression. Error bars represent standard deviation (SD).

In the second experiment and in contrast to anti-miR-21 inhibitor, pre-miR-21 precursor transfection failed again (Figure 14). In addition, even though anti-miR-21 inhibitor slightly increased the gene expression levels of all the other predicted targets,

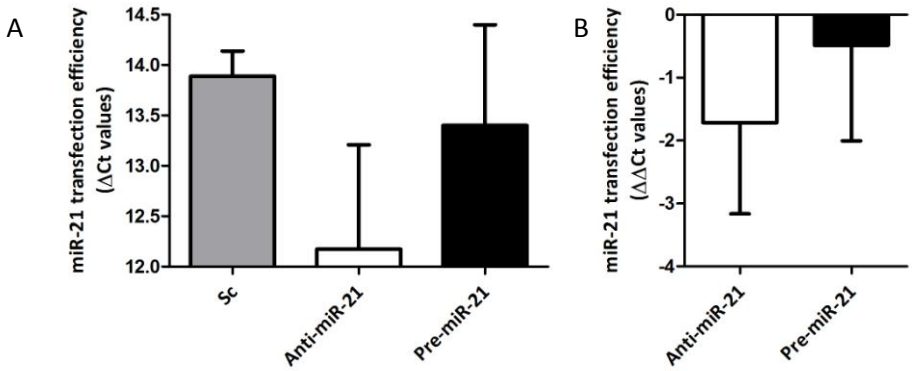

Figure 14 – miR-21 transfection efficiency in the second experiment. A) ΔCt values representation; B) ΔΔCt values representation, where Sc is the baseline (0). Error bars represent standard deviation (SD).

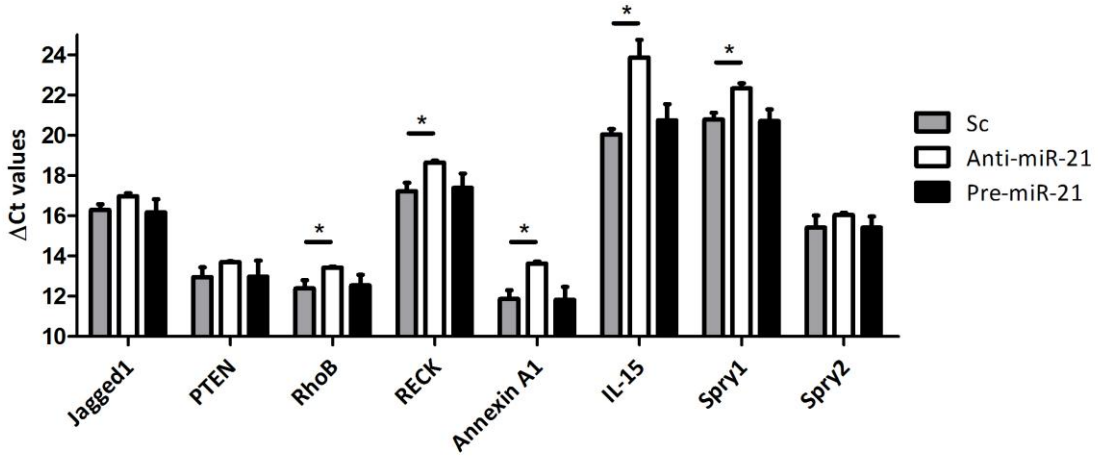

Figure 15 - Gene expression modulated by miR-21 levels for the second experiment. RhoB, RECK, Annexin A1, IL-15 and Spry1 were validated by the inhibition of miR-21 expression. Error bars represent standard deviation (SD).

only RhoB, RECK, Annexin A1, IL-15 and Spry1 were significantly validated (Figure 15).

Finally, in the third experiment, again in contrast to anti-miR-21 inhibitor that has slightly reduced miR-21 levels, pre-miR-21 precursor failed once again (Figure 16). Although the poor transfection efficiency, a small decrease of the miR-21 levels improves Jagged1, PTEN and Spry2 gene expression very slightly (Figure 17).

All these experimental results cannot be easily compared once they are from primary cultures which were obtained from different donors and thus may have different phenotypes. HUVECs are also notoriously difficult to transfect and the transfection rate is of about 40%, as previously assessed in the laboratory, accompanied by a high percentage of cell death caused by the electroporation. Moreover, in the analysis of miRNA levels, the choice of 18S as housekeeping gene, beyond U6, may have been a problem because, as 18S is an rRNA very abundant,

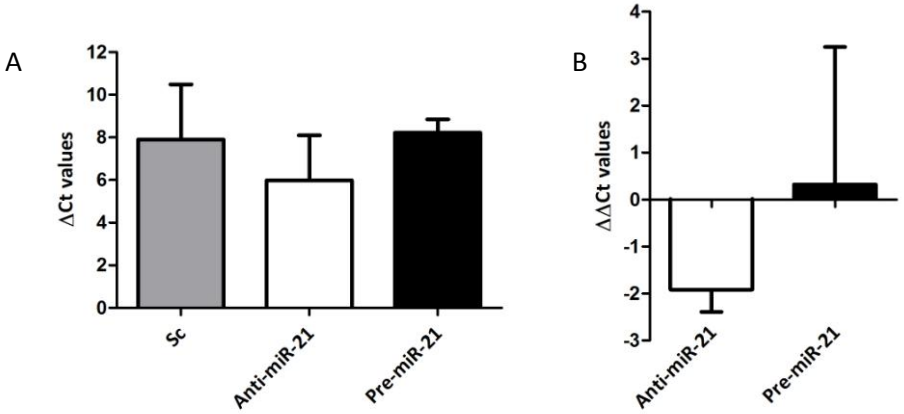

Figure 16 - miR-21 transfection efficiency in the third experiment. A) ΔCt values representation; B) ΔΔCt values representation, where Sc is the baseline (0). Error bars represent standard deviation (SD).

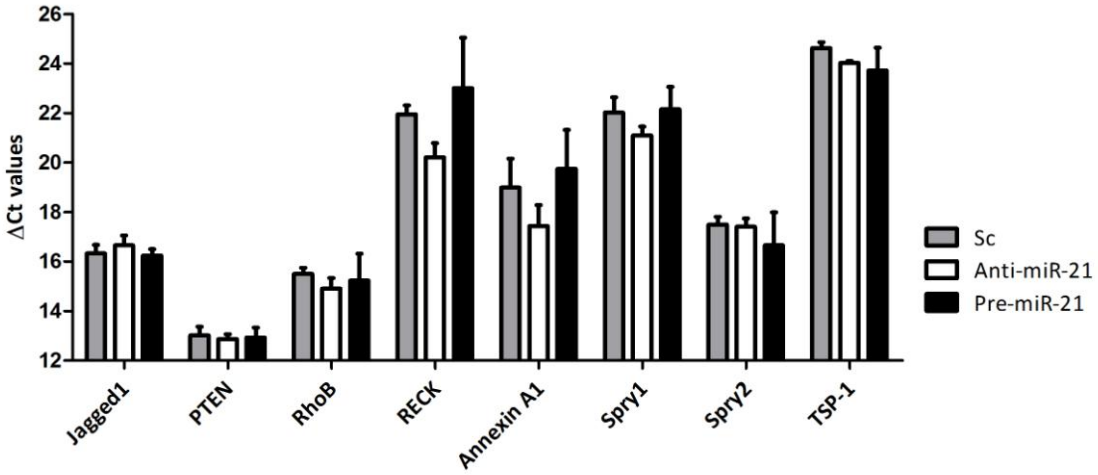

Figure 17 - Gene expression modulated by miR-21 levels for the third experiment. Error bars represent standard deviation (SD).

amplifying rapidly, it might have exhausted the reaction reagents making the detection of rare miRNA products difficult or even impossible.

As only PTEN and Spry2 had the most constant gene expression throughout these experiments, always being upregulated in the presence of reduced levels of miR-21, they were confirmed in a fourth experiment. Pre-miR-21 transfection again failed, but anti-miR-21 inhibitor worked (Figure 18), supporting this validation experiment (Figure 19). Thus, it may be concluded that, besides PTEN, Spry2 is a miR-21 target in HUVECs.

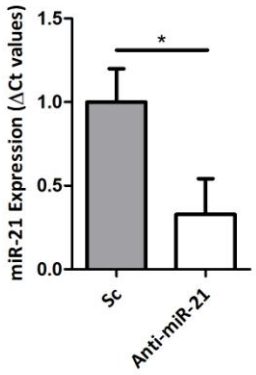

Figure 18 - miR-21 transfection efficiency in the confirmation experiment. ΔCt values representation. Error bars represent standard deviation (SD).

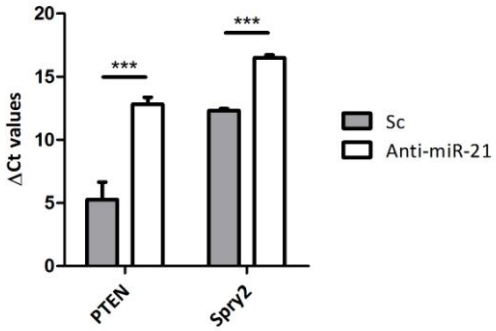

Figure 19 – Gene expression modulated by miR-21 levels for the confirmation experiment. Error bars represent standard deviation (SD).

Phenotypic changes modulated by miR-21 levels: Tube formation assay

In order to assess the capacity of HUVECs with high and low levels of miR-21 to form a vascular network, a matrigel assay was performed (Figure 20) as described in methods section.

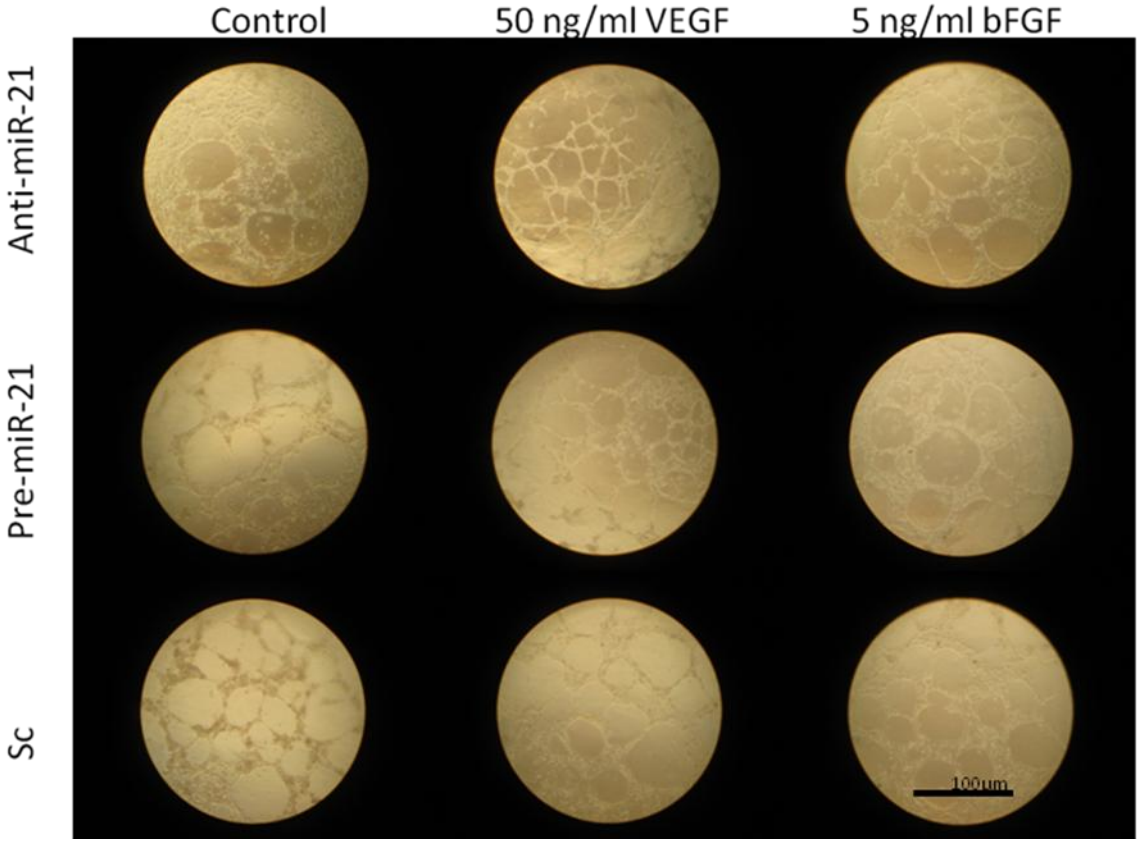

Figure 20 - Representative images of HUVEC tubules in growth factor-reduced Matrigel after transfection with anti-miR-21 inhibitor, pre-miR-21 precursor or scramble and culture for 24 hours in the respective conditions (50 ng/ml VEGF and 5 ng/ml bFGF).

Transfection with anti-miR-21 inhibitor, in contrast to pre-miR-21 precursor, did not work (Figure 21) for this particular experiment and for this reason, tube formation was quantified for pre-miR-21 condition (Figure 22). Only the thinnest tubes were counted, due to the fact that the larger ones may have been formed simply by cell deposition and adhesion to the matrix. This quantification demonstrates that mir-21 tends to increase tubulogenesis, in the presence of either angiogenic growth factor tested. Otherwise high levels of miR-21 seem to forfeit vascular network formation.

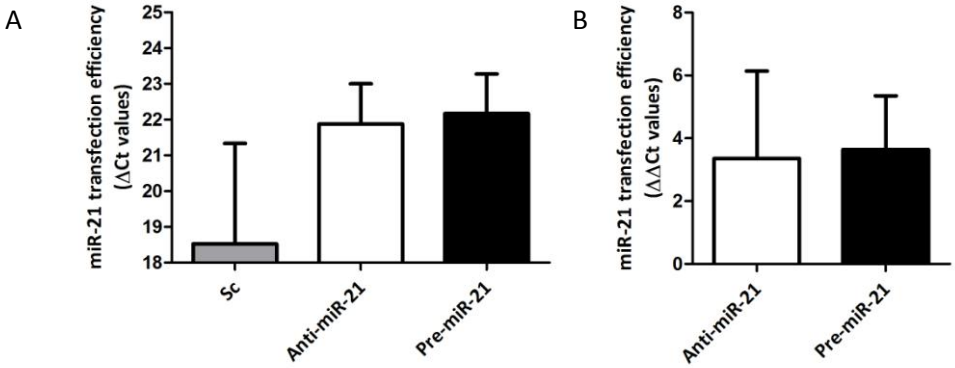

Figure 21 – miR-21 transfection efficiency for the matrigel assay. A) ΔCt values representation; B) ΔΔCt values representation, where Sc is the baseline (0). Error bars represent standard deviation (SD).

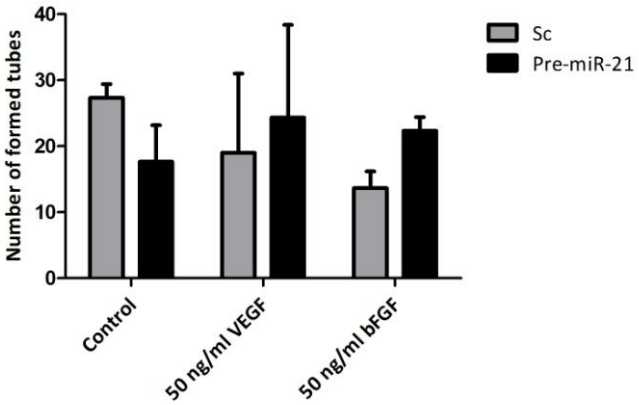

Figure 22 – Quantification of tube formation by transfected HUVECs in the presence of VEGF or bFGF. Error bars represent standard deviation (SD).

Phenotypic changes modulated by miR-21 levels: Cell migration assay

Cell migration was assessed through the "wound healing/scratch" assay as described in methods section. It is a simple and economical technique, in which upon creation of a gap called "scratch" on a confluent cell monolayer, the cells on the edge of the newly created gap will move toward the denuded area to close the wound until the cell-to-cell contacts are reestablished (Figure 23), similarly to migration of cells in vivo.

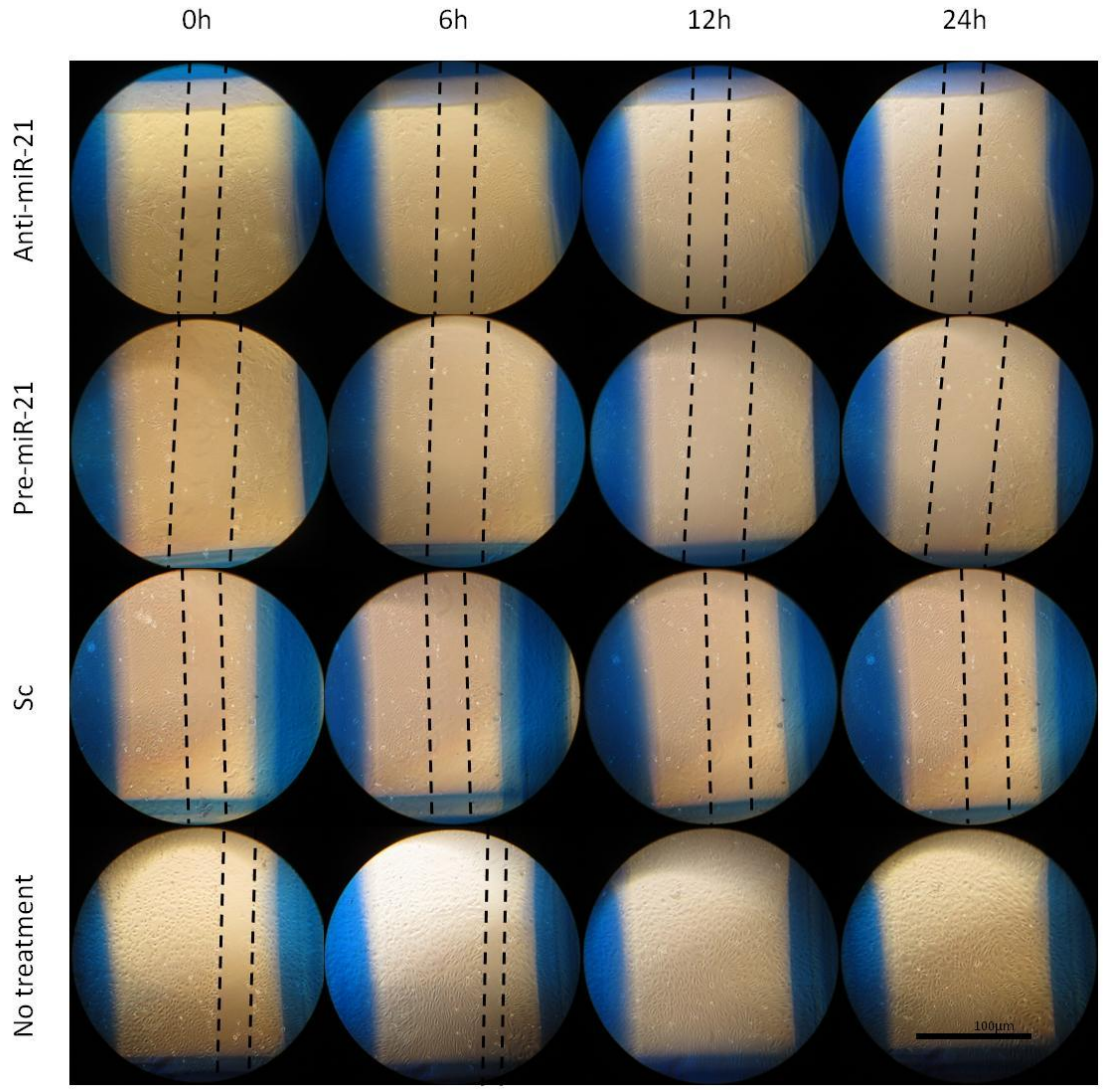

Figure 23 – Representative images of HUVEC migration capacity after transfection with anti-miR-21 inhibitor, pre-miR-21 precursor and scramble. Also the control without treatment is represented.

For the cell migration quantification, the condition in which miR-21 is overexpressed was not taken into account due to the transfection failure (Figure 24). For each of the other conditions, wound thickness was measured in different time points (Figure 25). Transfected HUVECs did not migrate clearly, in contrast to non treated cells that had already completely closed the wound after 12 hours. This is suggestive of transfection itself affecting cell migration.

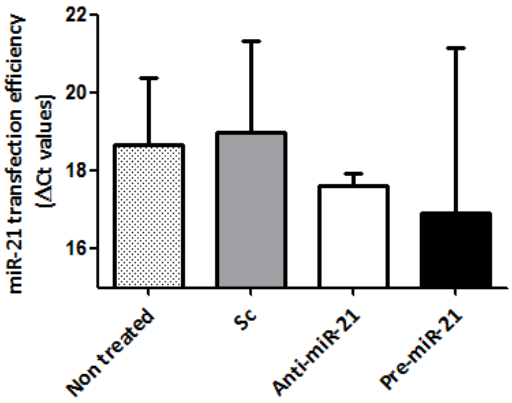

Figure 24 – miR-21 transfection efficiency for the scratch assay. ΔCt values representation. Error bars represent standard deviation (SD).

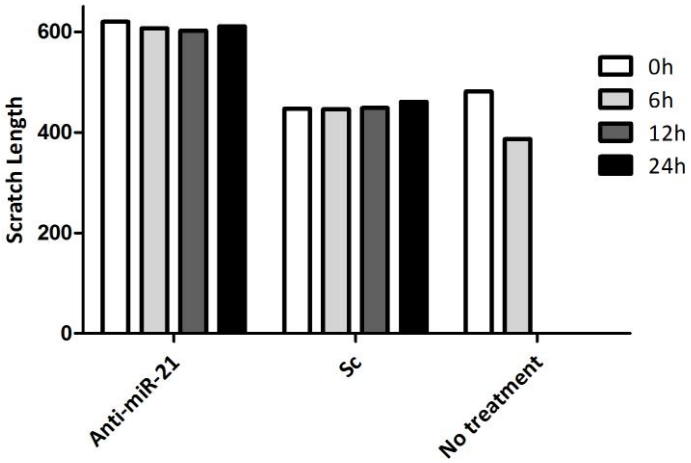

Figure 25 – Quantification of transfected HUVEC migration throughout time.

Endothelial-specific miR-21 KO mice generation

In order to evaluate miR-21 functions specifically on endothelial cells, we considered it would be very useful to generate endothelial-specific miR-21 knock-out (KO) mice to compare with wild type (WT) mice.

Therefore, miR-21 KO mice are being generated applying the bacteriophage P1-derived Cre/loxP recombination system to C57 Bl6 miR-21 conditional knock-out mice[81,82].

This system is highly effective and involves the Cre (*c*yclization *re*combination) enzyme, a type I topoisomerase that catalyzes the recombination between two loxP (*lo*cus of *X*-over of *P*1) sites, specific 34-base pair sequences that flank the gene coding region and 3'UTR in the conditional knock-out mice. These sites are acquired by homologous recombination in embryonic stem cells. Each loxP site comprises an asymmetric 8-base pair central spacer region that allows the recombination and confers directionality, flanked by two 13-base pair inverted repeats where Cre binds

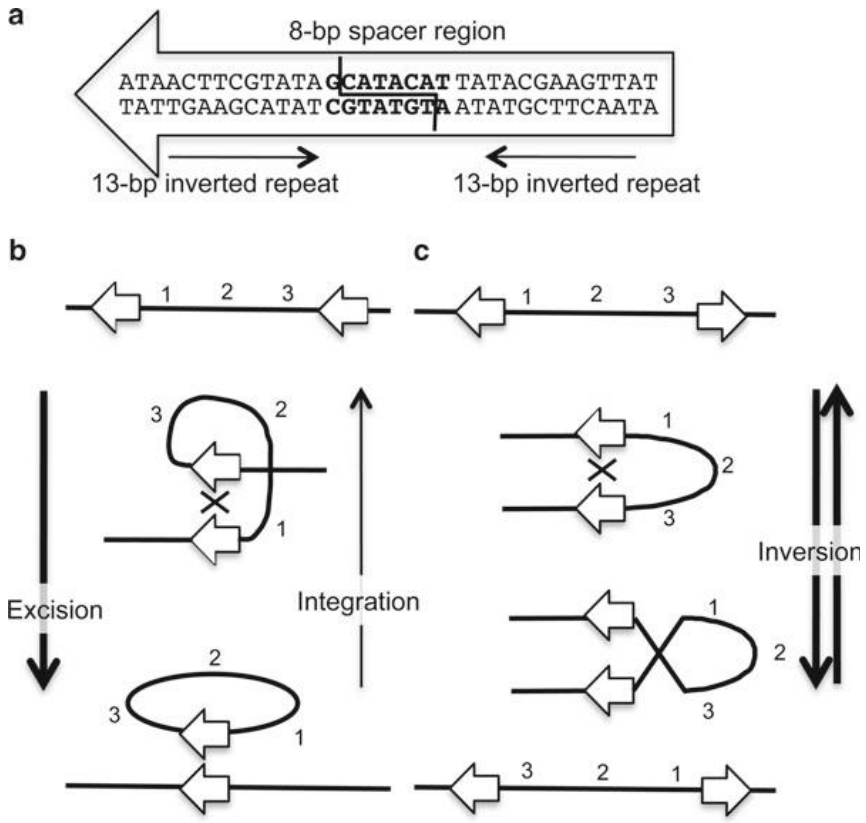

Figure 26 – Schematic representation of the Cre/lox recombination system. A) WT lox P sequence. The asymmetric spacer region states the direction of the lox P sequence, as showed by the arrow. b) Recombination between 2 lox P sites with the same direction. C) Recombination between 2 lox P sites in the opposite direction. Adapted from Morozov A. Controlled Genetic Manipulations. (1st edition). *Humana Press*, 2012.

to. The fusion of both loxP sites may result in excision, inversion or integration depending on the location and relative orientation of the loxP sites (Figure 26)[81,82].

To achieve tissue-specific knock-out of a gene, a tissue-specific promoter is recommended to be associated with the Cre transgene. For instance, vascular endothelial-cadherin (VE-Cadherin) promoter is required to have Cre expression specifically in endothelial cells under the regulatory control of VE-Cadherin[81,82].

Furthermore, for this system to be inducible, it makes use of a ligand-dependent chimeric Cre recombinase, called CreER^{T2} recombinase[83], which is a Cre fused with a mutated (G400V/M543A/L544A triple mutation) hormone-binding domain of the estrogen receptor (ER). Thus, it only will be active after treating mice with tamoxifen that is metabolized to the synthetic ER ligand 4-hydroxytamoxifen (OHT), which binds with high affinity to the ER ligand-binding domain of CreER^{T2} recombinase. The inducibility of this system allows external temporal Cre activity, limiting unwanted Cre activity and related side-effects[82].

The generation of genetically modified mice is assured by mice genotyping, which is designed to detect sequences in the murine genome by PCR amplification.

For this purpose, a set of PCR conditions has been developed to identify a detectable amplimer with any primers from sequences present only in a single copy in the genome. These primers must be about 30 nucleotides in length with approximately 50% guanosine or cytosine and they should not have homologous three prime ends, repetitive sequences or long runs of a single residue, while the amplimer must be 100-400 nucleotides in length, noting that shorter sequences amplify better[82].

So, firstly, miR-21 conditional KO mice were confirmed to be conditional (miR-21$^{lox/lox}$ mice) after some mice genotyping protocol optimizations. Several PCR conditions varying reagents quantities and annealing temperatures were tried, but only without lysis buffer and with the usual 0,5 µl of $MgCl_2$ at 60ºC (Figure 27) was

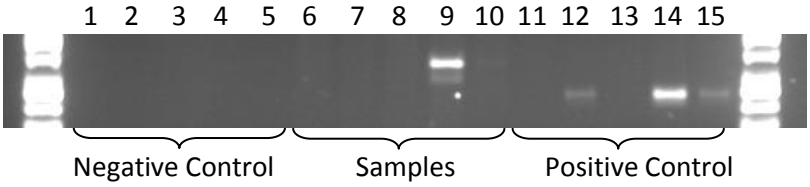

Figure 27 – Mice genotyping optimization test with various conditions at 60ºC. (1-5) Negative Control; (6-10) Sample; (11-15) Positive Control. (1,6,11) without lysis buffer with 0,25µl 40mM $MgCl_2$/sample; (2,7,12) 5µl lysis buffer with 0,25µl 40mM $MgCl_2$/sample; (3,8,13) (3,8,13) 5µl lysis buffer without $MgCl_2$; (4,9,14) without lysis buffer with 0,5µl 40mM $MgCl_2$/sample; (5,10,15) 10µl lysis buffer without $MgCl_2$.

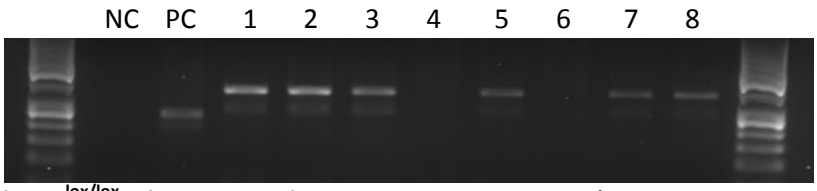

Figure 28 - miR-21$^{lox/lox}$ mice genotyping. NC – Negative Control; PC – Positive Control.

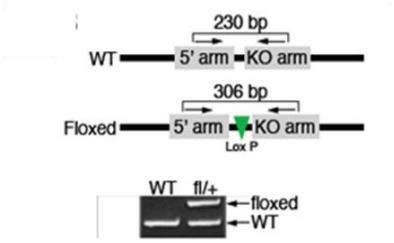

Figure 29 – Schematic representation of the genotyping PCR approach. The positions of the used primers are indicated by the arrows.

possible to genotype these mice (Figure 28).

In miR-21$^{lox/lox}$ mice genotyping, a WT allele is expected to have 230 pb while a floxed one is estimated to have 306 pb, as it includes the loxP site (Figure 29). CreER^{T2+} mice were also achieved by the deletion of floxed alleles of Dll4 conditional KO mice throughout some crosses between these and WT mice till obtain CreER^{T2+} mice WT for Dll4.

During mice genotyping, some differences were observed among the stains (Figure 30). EtBr has been chosen as the stain for nucleic acids, since it is very sensitive and stable. Despite that, it is a very cytotoxic and potent mutagen. GelRed, by contrast, is not cytotoxic neither mutagenic and it is designed to be impenetrable to latex gloves and even cell membranes. Though, while EtBr forms a straight band, GelRed seems to form a distorted one, which may difficult the interpretation of results when there is a very small distance between the bands (Figure 30).

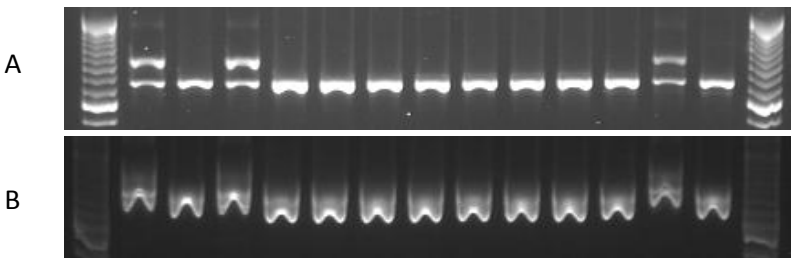

Figure 30 – Mice genotyping results obtained with (A) EtBr or (B) GelRed.

Once genotyped, these mice were bred together and then the resultant miR-21$^{lox/lox}$ CreER^{T2+} mice were selected and mated to be then induced by tamoxifen.

This procedure will give rise to endothelia miR-21 KO mice. These homozygous mutant mice present no overt abnormalities. Moreover, they exhibit less susceptibility to lung tumorigenesis due to K-ras activation through the upregulation of several antagonists of the Ras/MAP kinase signaling pathway[84].

Conclusions

In this study, it was demonstrated that HSCs express significantly less miR-21 than committed cells in general, including endothelial cells.

Moreover, bioinformatics approaches and literature allowed to choose 9 miR-21 predicted targets for further validation, namely Jagged1, annexin A1, IL-15, PTEN, RECK, RhoB, Spry1, Spry2 and TSP-1. Despite all these putative targets, only PTEN and Spry2 were validated to be modulated by the inhibition of miR-21 in HUVECs. Even so, there are indications of other predicted targets, whose levels seem to be determined by the reduction of miR-21 levels in these cells, such as Jagged1 and RhoB. However, the techniques employed for the validation of miR-21 predicted targets have had little success. This might be explained by the variation between HUVECs with different donor origin, the difficulty to transfect HUVECs or by the low transfection efficiency itself. It also can be explained by a possible exhaustion of the reaction reagents caused by the natural abundance of the housekeeping gene 18S, as well as the simple fact that miRNAs are particularly difficult to manage and to amplify due to their reduced size and rarity.

Furthermore, it was demonstrated that miR-21 tends to increase the formation of a vascular network in the presence of growth factors (VEGF or bFGF). In their absence, miR-21 appears to have the reverse effect. As regards the cell migration, no conclusions about miR-21 modulation were reached, because transfection seems to be affecting cell migration.

References

1. Marcelo KL, Goldie LC, Hirschi KK. Regulation of Endothelial Cell Differentiation and Specification. Circ Res 2013; 112(9): 1272-1287.
2. Bouïs D, Hospers GA, Meijer C, Molema G, Mulder NH. Endothelium in vitro: a review of human vascular endothelial cell lines for blood vessel-related research. Angiogenesis 2001; 4(2): 91-102.
3. Félétou M. The Endothelium. Part1: Multiple Functions of the Endothelial Cells – Focus on Endothelium-Derived Mediators. *Morgan & Claypool Life Sciences*, 2011.
4. Butler JM, Kobayashi H, Rafii S. Instructive role of the vascular niche in promoting tumour growth and tissue repair by angiocrine factors. *Nat Rev Cancer* 2010; 10(2): 138-146.
5. Suárez Y, Sessa WC. MicroRNAs As Novel Regulators of Angiogenesis. *Circ Res* 2009; 104: 442-454.
6. Urbich C, Kuehbacher A, Dimmeler S. Role of microRNAs in vascular diseases, inflammation, and angiogenesis. *Cardiovasc Res* 2008; 79: 581–588.
7. Liu LZ, Li C, Chen Q, Jing Y, Carpenter R *et al.* MiR-21 Induced Angiogenesis through AKT and ERK Activation and HIF-1α Expression. *PLoS ONE* 2011; 6(4): e19139.
8. Pan X, Wang ZX, Wang R. MicroRNA-21 A novel therapeutic target in human cancer. *Cancer Biol Ther* 2010; 10(12): 1224-1232.
9. Eble JA, Niland S. The extracellular matrix of blood vessels. *Curr Pharm Des* 2009; 15(12): 1385-400.
10. Hoffman GS, Weyand CM, Langford CA, Goronzy JJ. Inflammatory Diseases of Blood Vessels. (2nd edition). *Wiley-Blackwell*, 2012.
11. Ward JPT, Linden RWA. Physiology at a Glance. (3rd edition). *Wiley-Blackwell*, 2013.
12. Lizama CO, Zovein AC. Polarizing pathways: balancing endothelial polarity, permeability, and lumen formation. *Exp Cell Res* 2013; 319(9): 1247-1254.
13. Huang Z, Bao SD. Roles of main pro- and anti-angiogenic factors in tumor angiogenesis. *World J Gastroenterol*. 2004; 10(4): 463-470.
14. Lampugnani MG. Endothelial Cell-to-Cell Junctions: Adhesion and Signalling in Physiology and Pathology. *Cold Spring Harb Perspect Med* 2012; 2: a006528.
15. Lee CY, Bautch VL. Ups and downs of guided vessel sprouting: the role of polarity. *Physiology (Bethesda)*. 2011; 26(5): 326-333.
16. Prasain N, Stevens T. The actin cytoskeleton in endothelial cell phenotypes. *Microvasc Res* 2009; 77(1): 53–63.
17. Franke WW. Discovering the molecular components of intercellular junctions--a historical view. *Cold Spring Harb Perspect Biol* 2009; 1(3): a003061.
18. Michael M, Yap AS. The regulation and functional impact of actin assembly at cadherin cell–cell adhesions. Semin Cell Dev Biol 2013; 24(4): 298-307.
19. Mehta D, Malik AB. Signaling Mechanisms Regulating Endothelial Permeability. *Physiol Rev* 2006; 86: 279–367.
20. Ribatti D, Crivellato E. "Sprouting angiogenesis", a reappraisal. *Dev Biol* 2012; 372(2): 157-165.
21. Shi Y, Paluch BE, Wang X, Jiang X. PTEN at a glance. *J Cell Sci* 2012; 125: 4687-4692.
22. Manning BD, Cantley C. AKT/PKB Signaling: navigating downstream. *Cell* 2007; 129(7): 1261-1274.
23. Hooper AT, *et al*. Engraftment and reconstitution of hematopoiesis is dependent on VEGFR2-mediated regeneration of sinusoidal endothelial cells. *Cell Stem Cell* 2009; 4: 263–274.
24. Kobayashi H, Butler JM, O'Donnell R, Kobayashi M, Ding BS *et al.* Angiocrine factors from Akt-activated endothelial cells balance self-renewal and differentiation of haematopoietic stem cells. *Nat Cell Biol* 2010; 12(11): 1046-1056.

25. Ding BS, Nolan DJ, Butler JM, James D, Babazadeh AO *et al.* Inductive angiocrine signals from sinusoidal endothelium are required for liver regeneration. *Nature* 2010; 468(7321): 310-315.
26. Ding BS, Nolan DJ, Guo P, Babazadeh AO, Cao Z *et al.* Endothelial-derived inductive angiocrine signals initiate and sustain regenerative lung alveolarization. *Cell* 2011; 147(3): 539-553.
27. Ameres SL, Zamore PD. Diversifying microRNA sequence and function. *Nat Rev Mol Cell Biol* 2013; doi: 10.1038/nrm3611.
28. Santoro MM, Nicoli S. miRNAs in endothelial cell signaling: The endomiRNAs. *Exp Cell Res* 2013; 319(9): 1324-1330.
29. Chen X, Liang H, Zhang J, Zen K, Zhang CY. Secreted microRNAs: a new form of intercellular communication. *Trends Cell Biol* 2012; 22(3): 125-132.
30. Gramantieri L, Fornari F, Gallegari E, Sabbioni S, Lanza G *et al*. MicroRNA involvement in hepatocelular carcinoma. *J Cell Mol Med* 2008; 12(6A): 2189-2204.
31. Ambros V, Bartel B, Bartel DP, Burge CB, Carrington JC *et al.* A uniform system for microRNA annotation. *RNA* 2003; 9(3): 277-279.
32. Bentwich I. Prediction and validation of microRNAs and their targets. *FEBS Letters* 2005. 579: 5904-5910.
33. Thomas M, Lieberman J, Lal A. 2010. Desperately seeking microRNA targets. *Nat Struct Mol Biol* 2010; 17(10): 1169-1174.
34. Lai EC. Predicting and validating microRNA targets. *Genome Biol* 2004; 5(9): 115.
35. Shirdel EA, Xie W, Mak TW, Jurisica I. NAViGaTing the Micronome – Using Multiple MicroRNA Prediction Databases to Identify Signalling Pathway-Associated MicroRNAs. *PLoS One* 2011; 6(2): e17429.
36. Xiao F, Zuo Z, Cai G, Kang S, Gao X *et al.* miRecords: an integrated resource for microRNAs-target interactions. *Nucleic Acids Res* 2009; 37: D105-D110.
37. Dweep H, Sticht C, Pandey P, Gretz N. miRWalk - database: prediction of possible microRNA binding sites by "walking" the genes of 3 genomes. *J Biomed Inform* 2011; 44(5): 839-847.
38. van der Fits L, van Kester MS, Qin Y, Out-Luiting JJ, Smit F *et al.* MicroRNA-21 Expression in CD4+ T Cells is Regulated by STAT3 and Is Pathologically Involved in Sézary Syndrome. *J Invest Dermatol* 2011; 131: 762-768.
39. Wang K, Li PF. Foxo3a regulates apoptosis by negatively targeting miR-21. *J Biol Chem* 2010; 285: 16958-16966.
40. Du J, Yang S, An D, Hu F, Yuan W *et al.* BMP-6 inhibits microRNA-21 expression in breast cancer through repressing deltaEF1 and AP-1. *Cell Res* 2009; 19: 487-496.
41. Buscaglia LEB, Li Y. Apoptosis and the target genes of miR-21. *Chin J Cancer* 2011; 30(6): 371-380.
42. Gramantieri L, Fornari F, Gallegari E, Sabbioni S, Lanza G *et al*. MicroRNA involvement in hepatocelular carcinoma. *J Cell Mol Med* 2008; 12(6A): 2189-2204.
43. Donnem T, Fenton CG, Lonvik K, Berg T, Eklo K *et al.* MicroRNA Signatures in Tumor Tissue Related to Angiogenesis in Non-Small Cell Lung Cancer. *PLoS ONE* 2012; 7(1): e29671.
44. Krichevsky AM, Gabriely G. miR-21: a small multi-faceted RNA. *J Cell Mol Med* 2009; 13: 39-53.
45. McFall RC, Sery TW, Makadon M. Characterization of a new continuous cell line derived from a human retinoblastoma. *Cancer Res* 1977; 37: 1003-1010.
46. Bhandari A, Gordon W, Dizon D, Hopkin AS, Gordon E *et al.* The Grainyhead transcription factor Grhl3/Get1 suppresses miR-21 expression and tumorigenesis in skin: modulation of the miR-21 target MSH2 by RNA-binding protein DND1. *Oncogene* 2012; doi: 10.1038/onc.2012.168.

47. Ahmed MI, Mardaryev AN, Lewis CJ, Sharov AA, Botchkareva NV. MicroRNA-21 is an important downstream component of BMP signaling in epidermal keratinocytes. *J Cell Sci* 2011; 124: 3399-3404.

48. Marquez RT, Wendlandt E, Galle CS, Keck K, McCaffrey AP. MicroRNA-21 is upregulated during the proliferative phase of liver regeneration, targets Pellino-1, and inhibits NF-kβ signaling. *Am J Physiol Gastrointest Liver Physiol* 2010; 298: G535-G541.

49. Maccani MA, Avissar-Whiting M, Banister CE, McGonnigal B, Padbury JF *et al.* Maternal cigarette smoking during pregnancy is associated with downregulation of miR-16, miR-21, and miR-146a in the placenta. *Epigenetics* 2010; 5: 583-589.

50. Carletti MZ, Fiedler SD, Christenson LK. MicroRNA 21 Blocks Apoptosis in Mouse Periovulatory Granulosa Cells. *Biol Reprod* 2010; 83: 286-295.

51. Kim YJ, Hwang SJ, Bae YC, Jung JS. MiR-21 Regulates Adipogenic Differentiation through the Modulation of TGFβ Signaling in Mesenchymal Stem Cells Derived from Human Adipose Tissue. *Stem Cells* 2009; 27:3093-3102.

52. Patrick DM, Montgomery RL, Qi X, Obad S, Kauppinen S *et al.* Stress-dependent cardiac remodeling occurs in the absence of micro-RNA-21 in mice. *J Clin Invest* 2010; 120(11): 3912-3916.

53. Thum T, Gross C, Fiedler J, Fischer T, Kissler S *et al.* MicroRNA-21 contributes to myocardial disease by stimulating MAP kinase signalling in fibroblasts. *Nature* 2008; 456: 980-984.

54. Landgraf P, Rusu M, Sheridan R, Sewer A, Iovino N *et al.* A mammalian microRNA expression atlas based on small RNA library sequencing. *Cell* 2007; 129: 1401-1414.

55. Brooks BP, Paulson HL, Merry DE, Salazar-Grueso EF, Brinkmann AO *et al.* Characterization of an expanded glutamine repeat androgen receptor in a neuronal cell culture system. *Neurobiol Dis* 1997; 3: 313-323.

56. Salazar-Grueso EF, Kim S, Kim H. Embryonic mouse spinal cord motor neuron hybrid cells. *Neuroreport* 1991; 2: 505-508.

57. Velu CS, Baktula AM, Grimes HL. Gfi1 regulates miR-21 and miR- 196b to control myelopoiesis. *Blood* 2009; 19(113): 4720-4728.

58. Sugatani T, Vacher J, Hruska KA. A microRNA expression signature of osteoclastogenesis. *Blood* 2011; 117: 3648-3657.

59. Wu H, Neilson JR, Kumar P, Manocha M, Shankar P *et al.* miRNA Profiling of Naïve, Effector and Memory CD8 T Cells. *PLoS ONE* 2007; 2(10): e1020.

60. Benedito R, Roca C, Sörensen I, Adams S, Gossler A *et al*. The notch ligands Dll4 and Jagged1 have opposing effects on angiogenesis. *Cell* 2009; 137(6): 1124-1135.

61. Kume T. Novel insights into the differential functions of Notch ligands in vascular formation. *J Angiogenes Res* 2009; 1: 8.

62. Hashimi ST, Fulcher JA, Chang MH, Gov L, Wang S *et al.* MicroRNA profiling identifies miR-34a and miR-21 and their target genes JAG1 and WNT1 in the coordinate regulation of dendritic cell differentiation. *Blood* 2009; 114: 404-414.

63. Selcuklu SD, Donoghue MT, Kerin MJ, Spillane C. Regulatory interplay between miR-21, JAG1 and 17beta-estradiol (E2) in breast cancer cells. *Biochem Biophys Res Commun* 2012; 423(2): 234-239.

64. Bizzarro V, Petrella A, Parente L. Annexin A1: novel roles in skeletal muscle biology. *J Cell Physiol*. 2012; 227(8): 3007-3015.

65. Côté MC, Lavoie JR, Houle F, Poirier A, Rousseau S *et al*. Regulation of Vascular Endothelial Growth Factor-induced Endothelial Cell Migration by LIM Kinase 1-mediated Phosphorylation of Annexin 1. *J Biol Chem*. 2010; 285(11): 8013-21.

66. Angiolillo AL, Kanegane H, Sgadari C, Reaman GH, Tosato G. Interleukin-15 Promotes Angiogenesis in Vivo. *Biochem Biophys Res Commun*. 1997; 233(1): 231-237.

67. Armitage RJ, Macduff BM, Eisenman J, Paxton R, Grabstein KH. IL-15 has stimulatory activity for the induction of B cell proliferation and differentiation. *J Immunol*. 1995; 154(2): 483-490.

68. Weber M, Baker MB, Moore JP, Searles CD. MiR-21 is induced in endothelial cells by shear stress and modulates apoptosis and eNOS activity. *Biochem Biophys Res Commun*. 2010; 393(4): 643-648.

69. Reis ST, Pontes-Junior J, Antunes AA, Dall'Oglio MF, Dip N *et al*. miR-21 may acts as an oncomir by targeting RECK, a matrix metalloproteinase regulator, in prostate cancer. *BMC Urol*. 2012; 12: 14.

70. Gabriely G, Wurdinger T, Kesari S, Esau CC, Burchard J *et al*. MicroRNA 21 promotes glioma invasion by targeting matrix metalloproteinase regulators. *Mol Cell Biol*. 2008; 28: 5369–5380.

71. Connolly EC, Van Doorslaer K, Rogler LE, Rogler CE. Overexpression of miR-21 promotes an in vitro metastatic phenotype by targeting the tumor suppressor RHOB. *Mol Cancer Res*. 2010; 8(5): 691-700.

72. Liu M, Tang Q, Qiu M, Lang N, Li M. miR-21 targets the tumor suppressor RhoB and regulates proliferation, invasion and apoptosis in colorectal cancer cells. *FEBS Lett*. 2011; 585(19): 2998-3005.

73. Sabatel C, Malvaux L, Bovy N, Deroanne C, Lambert V *et al*. MicroRNA-21 exhibits antiangiogenic function by targeting RhoB expression in endothelial cells. *PLoS One*. 2011; 6(2): e16979.

74. Impagnatiello MA, Weitzer S, Gannon G, Compagni A, Cotten M *et al*. Mammalian Sprouty1 and 2 are membrane-anchored phosphoprotein inhibitors of growth factor signaling in endothelial cells. *J Cell Biol*. 2001; 152(5): 1087-1098.

75. Huebert RC, Li Q, Adhikari N, Charles NJ, Han X *et al*. Identification and regulation of Sprouty1, a negative inhibitor of the ERK cascade, in the human heart. *Physiol Genomics*. 2004; 18(3): 284-289.

76. Jung JE, Moon SH, Kim DK, Choi C, Song J *et al*. 2012. Sprouty1 Regulates Neural and Endothelial Differentiation of Mouse Embryonic Stem Cells. *Stem Cells Dev*. 2012; 21(4): 554-561.

77. hum T, Gross C, Fiedler J, Fischer T, Kissler S *et al*. MicroRNA-21 contributes to myocardial disease by stimulating MAP kinase signalling in fibroblasts. *Nature*. 2008; 456(7224): 980–984.

78. Sayed D, Rane S, Lypowy J, He M, Chen IY *et al*. MicroRNA-21 Targets Sprouty2 and Promotes Cellular Outgrowths. *Mol Biol Cell*. 2008; 19(8): 3272-3282.

79. Mei Y, Bian C, Li J, Du Z, Zhou H *et al*. miR-21 modulates the ERK-MAPK signaling pathway by regulating SPRY2 expression during human mesenchymal stem cell differentiation. *J Cell Biochem*. 2013; 114(6): 1374-1384.

80. Chen H, Herndon ME, Lawler J. The cell biology of thrombospondin-1. *Matrix Biol*. 2000; 19(7): 597-614.

81. Kühn R, Wurst W. Gene Knockout Protocols. (2nd edition). *Humana Press*, 2009.

82. Morozov A. Controlled Genetic Manipulations. (1st edition). *Humana Press*, 2012.

83. Monvoisin A, Alva JA, Hofmann JJ, Zovein AC, Lane TF *et al*. VE-cadherin-CreERT2 transgenic mouse: a model for inducible recombination in the endothelium. Dev Dyn 235:3413–22. *Dev Dyn*. 2006; 235(12): 3413-3422.

84. Patrick DM, Montgomery RL, Qi X, Obad S, Kauppinen S *et al*. Stress-dependent cardiac remodeling occurs in the absence of microRNA-21 in mice. *J Clin Inv*. 2010; 11(120): 3912-3916.